RESEARCH REPORT

RELAXATION DESIGN OF SEPARABLE
TUBE CONNECTORS

NAS-8-11523
Subcontract No. 63-30

to

ADVANCED TECHNOLOGY LABORATORIES
GENERAL ELECTRIC COMPANY

July 22, 1964

N66 39720

GPO PRICE $ _____

CFSTI PRICE(S) $ _____

Hard copy (HC) $3.00

Microfiche (MF) .75

ff 653 July 65

FACILITY FORM 602

(ACCESSION NUMBER) 85 (PAGES) CR-78959 (NASA CR OR TMX OR AD NUMBER)

(THRU) 1 (CODE) 15 (CATEGORY)

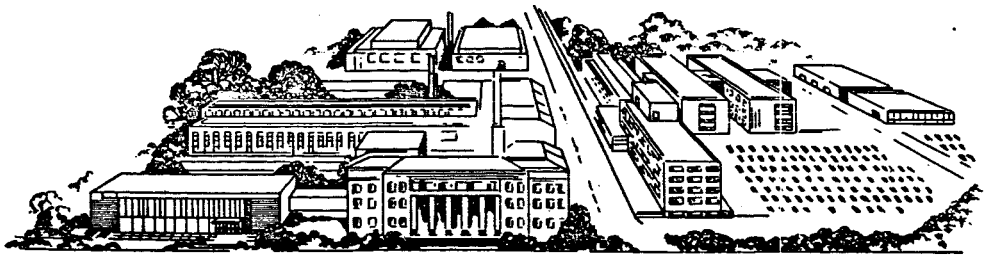

BATTELLE
MEMORIAL INSTITUTE

COT 40570

P. HAAS
R-PKVE-PMD
NASA - MSFC

RELAXATION DESIGN OF SEPARABLE TUBE CONNECTORS

NAS-8-11523
Subcontract No. 63-30

to

ADVANCED TECHNOLOGY LABORATORIES
GENERAL ELECTRIC COMPANY

July 22, 1964

by

L. M. Cassidy, E. C. Rodabaugh, D. B. Roach,
and T. M. Trainer

BATTELLE MEMORIAL INSTITUTE
505 King Avenue
Columbus, Ohio 43201

ABSTRACT

39720

A design procedure is developed for predicting the relaxation or time to leakage for separable tube connectors, including bolted-flanged and threaded types. The procedure is based upon the steady-state creep law, revised to account for the effects of primary creep. Sample calculations are provided for René 41 at 1500 F. The analysis includes the effects of external loads and temperature differentials. René 41 is selected as the best material currently available for use at 1440 F.

Author

TABLE OF CONTENTS

	Page
INTRODUCTION	1
SUMMARY	2
RECOMMENDATIONS	3
NOMENCLATURE	4
CREEP AND RELAXATION	6
MATERIALS	7
Introduction	7
Material Properties	7
Material Selection	11
Design Properties of René 41	15
DESIGN PROCEDURE	17
Basis for Design Procedure	17
Bolted-Flanged Connectors	17
Threaded Connectors	21
External Loads	24
Temperature Differentials	24
Retightening	25
Relaxation Data	25
Redesign Considerations	26
DISCUSSION OF SAMPLE CALCULATIONS	27
REFERENCES	29
APPENDIX A	
SAMPLE CALCULATIONS	A-1
Loose-Type Bolted Flange	A-1
Integral-Type Bolted Flange	A-4
Threaded Connector	A-5
External Loads	A-8
Bolt-Flange Temperature Differential	A-8
APPENDIX B	
DERIVATION OF EQUATIONS	B-1

TABLE OF CONTENTS
(Continued)

Page

Flange Flexibility B-1
Bolt Creep B-2
Flange Creep B-2
Intercept Stress Reduction B-3
Bolt Relaxation B-4
External Loads B-6
Bolt-Flange Temperature Differential B-7

APPENDIX C

SECONDARY EFFECTS C-1

Stress Concentrations C-1
Creep Bending of Bolt C-1
Dynamic Creep C-1
Gasket Creep C-2
Flange Rotations C-2

APPENDIX D

TUBE DESIGN D-1

LIST OF FIGURES

(Figures appear at end of report)

Figure 1. Typical Creep Curve

Figure 2. Steady-State Creep

Figure 3. Primary Creep

Figure 4. Creep-Relaxation Comparison (Copper at 165 C)

Figure 5. Master Creep Curve for René 41 Bar

Figure 6. Creep Rate of René 41 at 1440 F and 1500 F

Figure 7. Design Creep Properties of René 41

Figure 8. Typical Flange Geometry

Figure 9. Threaded Connector Model

Figure 10. Inwardly Projecting Flange

Figure 11. Loose-Type Flange Geometry (René 41-1500 F)

Figure 12. Integral-Type Flange Geometry (René 41-1500 F)

LIST OF FIGURES
(Continued)

Page

Figure 13. Residual Bolt Load Versus Time for Bolted-Flanged Connector (Shown in Figure 11)

Figure 14. Leakage Pressure Versus Time for Bolted-Flanged Connector (Shown in Figure 11)

Figure 15. Effect of Life Factor on Initial Stress (σ_{BT} = 65,400 psi)

Figure 16. Effect of Initial Bolt Stress on Relaxation (Flange Geometry of of Figure 11)

Figure 17. Threaded-Connector Geometry

Figure 18. Residual Nut Load Versus Time for Threaded Connector (Shown in Figure 17)

Figure 19. Intercept Stress Reduction

Figure 20. Creep of Flange and Bolt

Figure 21. Creep Bending of Rectangular Section (n = 6)

Figure 22. Combined Creep and Fracture Stress Range Diagram for 6.3% Mo-Waspaloy at 1500 F

LIST OF TABLES

Table 1. Nominal Compositions of Superalloys 9

Table 2. Properties of Superalloys at 1700 F 10

Table 3. Properties of Superalloys at 1400-1500 F 12

RELAXATION DESIGN OF SEPARABLE TUBE CONNECTORS

by

L. M. Cassidy, E. C. Rodabaugh, D. B. Roach,
and T. M. Trainer

INTRODUCTION

The design of separable tube connectors for operating below the temperature which produces significant creep of the metal used in the connector may be based on conventional elastic analysis methods. For example, the ASME Unfired Pressure Vessel Code[1]* gives a widely accepted method for designing bolted-flanged joints, including an approximation of the required bolt load and an elastic analysis of the flanges to insure adequate flange strength for carrying the required bolt load.

Even at temperatures where creep does not occur, the design of a conventional separable tube connector is not simply a strength problem, since the usual criterion of failure is leakage and leakage may occur without necessarily overstressing any part of the connector. In practice, conventional connectors are initially loaded (tightened bolts in a bolted-flanged connector, tightened nut in a threaded connector) so that the elastically stored forces in the connector are sufficient to prevent separation of the connector parts due to the subsequently applied service loads arising from internal pressure or loads on the attached pipe or tubing. Accordingly, not only the stresses but also the strains or displacements are significant in connector design.

At operating temperatures where significant creep occurs, the design method for the connector must take into account the relaxation of the elastically stored forces which occur as a result of the plastic flow of the metal components. In bolted-flanged joints designed in accordance with the ASME Code[1], this relaxation effect is taken into account in an indirect and approximate manner by the use of allowable stresses which are based on creep or stress-to-rupture properties of the material. These allowable stresses, however, do not necessarily reflect the relaxation characteristics of bolted-flanged joints in general, and use of the method may result in excessively conservative design or inadequate performance over the desired service life.

There have been previous discussions and simplified analyses[2,3,4,5,6,7] of relaxation in bolted joints. Unfortunately, a practical solution considering primary creep does not appear to have been developed. The method of analysis presented in this report is intended as a workable approach to the design of separable tube connectors at temperatures where creep or relaxation occurs.

The only known published data on the elevated-temperature testing of separable connectors in order to study leakage is a very comprehensive set of tests[8,9,10] by the British Pipe Flanges Research Committee on bolted-flanged joints. The results of these tests indicate a definite relation between the time to leakage and the temperature. However, the results are not amenable to a theoretical analysis because of the lack of sufficient specimen creep or relaxation data on the materials used in the test.

*Numbers in raised parentheses designate References on page 29.

Material properties are, of course, interrelated with the design procedure. Accurate information of material properties (such as yield strength, modulus of elasticity, and creep or relaxation rates) are needed to apply the design procedure. Accordingly, this report includes a discussion of material properties and tabulation of properties for various materials with desirable high-temperature properties. The section of the report on material properties leads to a selection of an optimum material for use in connector design for aerospace application at 1440 F operating temperature.

SUMMARY

Materials were evaluated for use at 1440 F, with the result that René 41 is the material choice for the connector design. René 41 is equivalent in strength to the other candidate materials at 1440 F, and has a greater amount of data available. In addition, René 41 is readily available and has seen considerable research and service experience. Nevertheless, the lack of a suitable family of creep curves at 1440 F led to the recommendation that creep or relaxation data be generated for René 41.

With the expectation that relaxation data will not be available for most materials, the design method is directed primarily toward the utilization of creep data, with a discussion on the use of relaxation data. The widespread scatter in creep data as well as possible secondary effects, such as those discussed in Appendix C, led to the use of a design factor of safety.

The design procedure utilizes the steady-state or power law of creep with an assumed zero time reduction in stress to account for primary creep. This approach is conservative for short times, the degree of conservatism depending upon the amount of primary creep exhibited by the material at the design temperature. A comparison is shown for predicting relaxation from creep data for various creep theories.

Both bolted-flanged and threaded connectors are included in the relaxation design, and sample calculations are provided to illustrate the design method for each type of connector. The effect of temperature differentials and external loads on the leakage pressure* is considered. Secondary effects such as stress concentrations, creep bending of bolt, dynamic creep, gasket creep, and flange rotations are discussed briefly, but are not included as an integral part of the design procedure.

The design method is suitable for hand calculations, but could be expedited and easily adapted for solution on a high-speed computer. The optimum (minimum weight) design for a given value of leakage pressure can be determined only after calculating a wide range of geometries. A suitable number of calculations enables the static** design to be rated in accordance with various combinations of leakage pressure and time. The detailed gasket design is not considered herein, since Reference (11) is quite comprehensive in this respect.

*Leakage pressure refers to the value of uniform internal pressure at or below which tolerable leakage rates occur, and should not be confused with the value of gasket pressure required for (1) initially seating the gasket or (2) residual pressure required on the gasket in order to prevent excessive leakage rates. The determination of these gasket pressures is not covered in this report.

**Static design refers to a conventional-type design such as the ASME Boiler Code[1], which is not time dependent.

Various methods of analyses are discussed for the creep design of tubes. The data available indicate that a suitable approach for the tube design is to design for the tangential (hoop) stress on the basis of uniaxial tensile creep data.

RECOMMENDATIONS

On the basis of the subject design study, the following recommendations are made in support of the over-all design effort for separable tube connectors:

(1) Creep and/or relaxation data on René 41 at 1440 F, preferably relaxation data, should be generated.

(2) It is recommended that a design factor of safety of 2.0 be used. However, one or more René 41 connectors should be tested at 1440 F in order to substantiate this factor of safety.

(3) Avoid yielding of the connector components due to stresses incurred during installation.

(4) Even though retightening of the connector compensates for the bolt or nut relaxation, care must be taken not to incur excessive deformations in the component parts which could lead to rupture.

(5) In order to be conservative, the cycle time should be measured from the start of the heating cycle to the end of the cooling cycle.

(6) Consideration should be given to various design configurations. For example, loose-type bolted flanges may offer certain advantages over integral-type flanges which would not be realized in a static design.

NOMENCLATURE*

α = mean coefficient of thermal expansion, in/in/°F

A = area of bolt, gasket, tube, or flange, in.

c = inner radius of flange or tube, in.

C_1 = coefficient in steady-state creep law

C_2 = coefficient in intercept stress law

d = outer radius of flange or tube, in.

δ = deflection, in.

e = moment arm for flange bending, in.

ϵ = normal strain, in/in.

$\dot{\epsilon}$ = strain rate = $\frac{de}{dt}$, in/in/hr

E = modulus of elasticity, psi

F_B = bolt flexibility, in/lb

F_B' = bending flexibility of the "bolt" (threaded connector), in/lb

F_F = flange flexibility at bolt circle, in/lb

F.S. = design factor of safety

g = radius to centerline of gasket, in.

h = flange thickness, in.

θ = rotation, radians

K_B = creep rate of bolts, in/hr

K_B' = bending creep rate of the "bolt" (threaded connector), in/hr

K_F = creep rate of flanges, in/hr

L = influence coefficient from Page 138, Paragraph UA-47, of the ASME Code[1]

L_B, L_F = effective length of bolt and flange, respectively, in.

m = exponent in intercept stress law

*The nomenclature of the ASME Code[1] is used exclusively in the sample Code calculations on pages A-1 and A-4, and is used elsewhere in the report where necessary for clarity.

M = flange bending moment = Pe, in-lb

ν = Poisson's ratio

n = exponent in steady-state creep law

p = uniform internal pressure, psi

P = total bolt load, lb

P_t' = design value for residual bolt load = $\frac{P_t}{F.S.}$, lb

r_F = flexibility ratio = F_F/F_B

r_F' = flexibility ratio = F_B'/F_B

r_K = creep ratio = K_F/K_B

r_K' = creep ratio = K_B'/K_B

R = life factor = $\frac{1 + r_F}{1 + r_K}$ (bolted-flanged connector) or $\frac{1 + r_F + r_F'}{1 + r_K + r_K'}$ (threaded connector)

σ = normal stress, psi

t = time, hr

ΔT = temperature differential, °F

V = influence coefficient from Figure UA-51.3, Page 144, Paragraph UA-51 of the ASME Code[1]

w = width of gasket, in.

Subscripts

A = axial load

B = bolt

c = creep

e = elastic

F = flange

G = gasket

M = bending moment

o = intercept or zero time

r = radial direction in tube

R = room temperature

t = time

T = tube or design temperature

ϕ = circumferential direction in tube

y = yield

z = axial direction

CREEP AND RELAXATION

Creep and relaxation are closely related, even though they are not necessarily interchangeable in a stress-analysis problem. These phenomena play an important role in the behavior of a separable connector operating at elevated temperatures, and are best illustrated by mechanical models.

Creep is the tendency for a material to exhibit time-dependent strains at a constant stress level, typical of metals at elevated temperatures. Figure 1 shows a typical creep curve (neglecting tertiary creep) and the corresponding Maxwell-Kelvin model. Figure 1 is obtained by superposition of the Maxwell and Kelvin models of Figures 2 and 3, representing the steady-state and primary creep, respectively. The enclosed design procedure utilizes an equivalent Maxwell model, shown as the dashed curve in Figure 1. The total strain is made up of an instantaneous strain and a time-dependent (steady-state) strain. The instantaneous or intercept strain ϵ_o includes the elastic strain ϵ_e plus an additional strain $C_2\sigma_o^m$ which conservatively accounts for the primary creep period.

Relaxation is the reduction or relaxation of stress in time under a constant strain. Elastic strains are replaced by creep strains, causing a progressive reduction in stress. The models in Figures 1-3 can be considered relaxation models by assuming a constant total strain rather than a constant stress.

There has been considerable literature written on how to predict relaxation from creep data, few agreeing on the best creep theory to use. Although there are very few test data available on the same material to enable a comparison of various theories, Finnie and Heller[7] made a comparison of copper at 165 C with an initial stress of 13,500 psi. Figure 4 shows that the steady-state creep law with the intercept stress reduction used herein is conservative for short times and shows good agreement with the experimental results for longer times. Of course, the time scale would be quite reduced for a superalloy at 1440 F.

The most basic form of a separable connector would be flexible bolting in a pair of rigid flanges, in which case the model of Figure 1 would suffice for a relaxation analysis. The tightness of the joint would be dependent on the ability of the bolt to resist creep deformations. However, the flange assembly can also be represented by a Maxwell model in parallel with the bolt assembly. The flange can increase or decrease the rate of bolt relaxation, depending upon the characteristics of the flange geometry. A properly designed flange assembly should be superior to a rigid flange in that the flange elastic recovery as a spring will retard the bolt relaxation.

MATERIALS

At the initiation of the program, it was thought that the connector might be exposed to service temperatures in the range from 70 F to a maximum of 1700 F. The upper temperature limit was subsequently changed to 1440 F. Consequently, material properties are evaluated at both 1700 F and 1440 F, and a material selection made at 1440 F.

Introduction

At the initiation of the materials survey, it was apparent that certain material properties were of major importance in establishing the optimum connector design. Strength over the desired temperature range was the prime criterion. In addition, because of the continued requirement to design space vehicles with minimum weight, density (or strength-to-density ratio) was a major consideration. Also, because service conditions involve cycling from maximum temperature to room temperature, thermal shock, embrittlement, and oxidation were also considered important criteria.

Of the various strength parameters, creep strength and resistance to relaxation were considered of utmost importance. In the installation of a separable connector, the connector is tightened to a given stress. To prevent leakage during service, this stress should remain sufficiently high during service. Relaxation or creep during service will tend to loosen the joint and may give rise to leakage. In addition, good rupture strength and ductility are deemed necessary to insure against complete, catastrophic failure of the connector. Also, because the connector will be installed and tightened at room temperature, consideration must be given to thermal expansion of the connector during heating to the maximum temperature. Variations in thermal expansion of different materials comprising the tubing and the connector could lead to tightening of the connector and undue stress, or to loosening of the connector and leakage.

In addition, consideration was given to the availability, fabricability, machinability, and weldability of the various candidate materials. Of particular importance was the general engineering "know-how" in the handling and use of the various alloys. Finally, since the connector should be capable of being loosened or tightened periodically, consideration was given to bonding or self-welding of the various candidate materials under service conditions.

Material Properties

As indicated above, candidate alloys for separable connectors must have good creep, rupture, and relaxation strengths over the anticipated service-temperature range. Good resistance to thermal shock, oxidation, and embrittlement during cyclic service is also required. These requirements are almost identical to those involved in selection of alloys for turbine-bucket application in aircraft gas turbines. Turbine-bucket materials, however, are not selected on the basis of relaxation resistance, although rupture strength and creep resistance are major requirements. At the present time, turbine-bucket materials are selected on the basis of rupture strength and

thermal-shock resistance. Thus, it was evident that the requirements for separable connectors were sufficiently similar to those of turbine buckets that a summary of the various turbine-bucket materials would likely yield those alloys having the most desired combination of properties for the design of high-temperature separable connectors.

A survey of published property data for various nickel- and cobalt-based superalloys was conducted. Emphasis was placed on creep and rupture strength at 1700 F, and on short-time tensile properties over the service-temperature range. A search of the literature revealed that relaxation data were not available for the bulk of the alloys of interest. On the basis of this survey, the following alloys were selected for more thorough examination:

Wrought Alloys

(1) Astroloy
(2) Nimonic 105
(3) Nimonic 115
(4) René 41
(5) Udimet 700
(6) Unitemp 1753
(7) Waspaloy

Cast Alloys

(8) GMR 235
(9) IN-100
(10) Inco 713C
(11) Nicrotung
(12) SM 200
(13) SM 302
(14) SM 322

These alloys have the highest strength at 1700 F. All have been, or, are being considered for use as turbine buckets in gas-turbine engines. Not all of these alloys are readily available, and not all are weldable.

In addition, three more common, lower strength superalloys on which extensive experience in fabrication and usage is available were studied for comparison purposes. These were:

(15) Inconel X
(16) N 155
(17) S 816

Typical compositions for these 17 alloys are given in Table 1.

Alloys for Use at 1700 F

The typical properties of the 17 candidate alloys are given in Table 2. It will be noted in this table that short-time tensile and rupture data were available for the bulk of the alloys. Creep data at 1700 F were quite often lacking. Where creep data were

TABLE 1. NOMINAL COMPOSITIONS OF SUPERALLOYS

Alloy	Form		C	Cr	Co	Fe	Ni	Mo	W	Al	B	Ti	Zr	Other
	Wrought	Cast												
Astroloy	X		0.10	15.0	15.5	–	Balance	5.0	–	4.2	0.03	4.0	–	–
Nimonic 105	X		0.15	15.0	20.0	–	Balance	5.0	–	4.7	–	1.2	–	–
Nimonic 115	X		–	–	–	–	–	–	–	–	–	–	–	–
Rene' 41	X		0.09	19.0	–	–	Balance	10.0	–	1.5	0.005	3.5	–	–
Udimet 700	X	X	0.10	15.0	18.5	–	Balance	5.2	–	4.3	0.008	3.5	–	–
Unitemp 1753	X		0.24	16.0	7.5	9.5	Balance	1.6	8.4	1.9	0.008	3.2	0.06	–
Waspaloy	X		0.08	19.0	13.5	–	Balance	4.5	–	1.3	0.008	3.0	0.08	–
GMR-235		X	0.14	16.0	–	10.0	Balance	5.5	–	3.0	0.05	2.0	–	–
IN 100		X	0.18	10.0	15.0	–	Balance	3.0	–	5.5	0.015	5.0	0.05	–
Inco 713C		X	0.14	12.0	–	–	Balance	4.5	–	6.0	0.012	0.5	0.05	2.0 Cb
Nicrotung		X	0.10	12.0	10.0	–	Balance	–	8.0	4.0	0.05	4.0	0.05	–
SM-200		X	0.15	9.0	10.0	1.5	Balance	–	12.5	5.0	0.015	2.0	0.05	1.0 Cb
SM-302		X	0.85	21.5	Balance	0.8	–	–	–	10.0	0.005	–	0.2	9.0 Ta
SM-322		X	1.00	21.5	Balance	1.5	–	–	–	9.0	–	0.75	2.25	4.5 Ta
inconel X	X		0.06	16.0	–	7.0	Balance	–	–	0.60	–	2.5	–	1.0 Cb
N-155	X	X	0.15	21.0	20.0	Balance	20.0	3.0	–	–	–	–	–	1.0 Cb + 2.5 V
S-816	X		0.40	20.0	44.0	Balance	20.0	4.0	4.0	–	–	–	–	4.0 Cb

TABLE 2. PROPERTIES OF SUPERALLOYS AT 1700 F

Alloy	0.2% Yield Strength, ksi							Elongation, %, at 1700 F	Stress Rupture, ksi, for Indicated Hours at 1700 F			Creep, %	Stress, ksi, for Indicated % Creep and Indicated Hours at 1700 F			Modulus of Elasticity, ksi x 10^{-6}			Coefficient of Thermal Expansion, in./in./F x 10^{-6}			Density, lb/cu in.
	R.T.	1000 F	1200 F	1400 F	1600 F	1700 F	1800 F		10	100	1000		10	100	1000	1600 F	1700 F	1800 F	80 to 1600 F	80 to 1700 F	80 to 1800 F	
Astroloy (W)	157	153	148	140	–	–	–	–	–	24	14	–	–	–	–	22	20	16.7	–	–	–	0.286
Nimonic 105 (W)	–	132[a]	144[b]	–	58[f]	–	24[g]	–	–	24[f]	13.5[f]	–	–	–	–	–	–	–	–	–	–	–
Nimonic 115 (W)	122	118	119	113	82	64	–	10	37	24.5	16.5	1.0	35	21.5	13	–	–	–	8.9	9.2	9.6	0.284
Rene' 41 (W)[j]	120	117	116	107	70	46	–	29	25	8	–	0.2	17	14	–	23.0	22.0	–	8.7	9.0	9.3	0.298
Rene' 41 (W)[k]	154	146	144	136	80	50	–	26	23	12	–	0.2	13	10	–	23.0	22.0	–	8.7	9.0	9.3	0.298
Udimet 700 (W)	140	–	124	120	92	68	44	31	40	28	16	1.0	27.3	17.5	9.6	21.5	19.7	17.5	8.9	9.3	9.6	0.287
Unitemp 1753 (W)	129	126	128	120	90	62	–	21	–	18.5	12	1.0	33[f]	23[f]	–	22.8[i]	21.9[i]	20.4[i]	8.2	8.6	–	0.305
Waspaloy (W)	115	106	100	99	76	50	–	35[e]	32[f]	18[f]	12[f]	1.0	36[d]	25[d]	14[d]	20	18.5	17	9.1	9.3	9.7	0.296
GMR-235 (C)	102	94	89	78	40	30	–	–	28	18	13	1.0	20	9	–	21.7	20.7	19.5	8.5	8.8	9.1	–
IN 100 (C)	123	123	123	120	108	80	61	5	54	38	27	–	–	–	–	–	–	–	–	–	–	0.275
Inco 713C (C)	105	104	104	103	89	62	48	10	–	30	23	0.2	8	6	4	22	–	–	8.7	8.9	9.2	0.286
Nicrotung (C)	120	106	102	96	77	64	52	4.5	43	32	20	–	–	–	–	25.7[i]	25[i]	–	8.3	8.5	8.8	0.300
SM-200 (C)	120	124	125	123	109	87	67	3.5	52	40	–	–	–	–	–	–	–	–	–	–	–	0.304
SM-302 (C)	100	74	66	56	45	39	33	13.5	26	18.5	13.5	–	–	–	–	–	–	–	8.3	8.5	8.7	0.333
SM-322 (C)	91	63	57	51	–	–	–	–	32	28	21	–	–	–	–	–	–	–	8.3	8.5	8.7	0.322
Inconel X (W)	90	88	80	70	30	20	–	–	–	8	3	1.0	16[e]	12[e]	–	20[c]	–	–	9.2	–	–	0.298
N-155 (W)	57	48	43	36	25	–	–	–	17.5[f]	10[f]	7.3[f]	–	–	–	–	21	–	–	10.0	10.1	10.2	0.300
S-816 (W)	55	46	44	40	35	–	22	18.5	23[e]	16[e]	9[e]	–	9.8[e,h]	–	–	26[e,i]	–	–	8.8	8.9	9.0	0.313

Note: W = wrought; C = cast.

(a) 930 F.
(b) 1290 F.
(c) 1400 F.
(d) 1500 F.
(e) 1600 F.
(f) 1650 F.
(g) 1830 F.
(h) 0.001%/hr.
(i) Dynamic.
(j) Sol. tr. 2150 F, 2 hr; AC. Aged 1650 F, 4 hr; AC.
(k) Sol. tr. 1950 F, 4 hr; AC. Aged 1400 F, 16 hr; AC.

not available at 1700 F, information on the creep strength at lower temperatures was included.

On the basis of yield strength at 1700 F and creep and rupture strengths at 1700 F, it is evident in Table 2 that the cast alloys have significantly higher strength than the wrought alloys. Of the 17 candidate alloys, SM 200, IN 100, Nicrotung, and Udimet 700 are the highest strength alloys at 1700 F. Of these only Udimet 700 is a wrought material. Of the wrought materials, the order of decreasing strength at 1700 F may be listed as Udimet 700, Nimonic 115, Unitemp 1753, René 41, and Waspaloy.

In general, it was found that the cobalt-based alloys were of lower strength than the nickel-based alloys.

It will be noted that the coefficients of thermal expansion of these alloys were quite similar in the temperature range from 1600 to 1800 F. Likewise, the density values for the nickel-base alloys were quite similar. Those alloys containing significant amounts of tungsten, of course, had slightly higher density values than those containing little tungsten. Because the density values were so similar, there was little merit in comparing the alloys on a strength-to-density basis.

Alloys for Use at 1440 F

It was subsequently decided that the maximum operating temperature for the connector should be reduced from 1700 to 1440 F. Consequently, a survey of the properties of the 17 alloys listed in Table 1 was made to ascertain the most promising alloys at this reduced temperature. The properties of the alloys at 1400 and 1500 F are summarized in Table 3. Where possible, values at 1440 F were interpolated.

The data given in Table 3 show that the wrought alloys compare more favorably with the cast alloys at this temperature than they did at 1700 F. It will be noted that on the basis of yield strength at 1400 to 1500 F, René 41 and Astroloy (Udimet 700) compare favorably with SM 200 and IN 100. On the basis of stress for rupture in 10 hours at 1400 F, SM 200, Udimet 700, Nimonic 115, and René 41 have very similar strengths. For longer times at 1400 F and at 1500 F, René 41 compares less favorably with these other alloys. It will be noted that at 1500 F and above, Waspaloy has strength properties equal to René 41. In the range of 1400 to 1500 F, René 41 has appreciably better short-time tensile properties and higher short-time (10-hour) rupture and creep strengths than Waspaloy.

Material Selection

On the basis of the material properties cited in the preceding section, SM 200, Udimet 700, Nimonic 115, IN 100, and René 41 appear to have the highest strength at 1440 F. SM 200 is a cast alloy which is used principally as the turbine bucket material in the J57 engine. Extensive experience in its use and handling has not been gained as yet. In addition, it is not normally considered a weldable alloy. Udimet 700 has gained appreciable usage, and many shops are familiar with forging and machining the alloy. It is not readily rolled and is not considered weldable. The Nimonics are British alloys not readily available in the United States, and extensive data and experience are not

TABLE 3. PROPERTIES OF SUPERALLOYS AT 1400-1500 F

Alloy	0.2% Yield Strength, ksi			Elongation, %			Stress Rupture, ksi: Hours at 1400 F			Stress Rupture, ksi: Hours at 1500 F			Creep, %	Stress for Indicated % Creep, ksi: Hours at 1400 F			Stress for Indicated % Creep, ksi: Hours at 1500 F			Modulus of Elasticity, ksi x 10^{-6}			Coefficient of Thermal Expansion, in./in. F x 10^{-6}		
	1400 F	1440 F	1500 F	1400 F	1440 F	1500 F	10	100	1000	10	100	1000		10	100	1000	10	100	1000	1400 F	1440 F	1500 F	1400 F	1440 F	1500 F
Astroloy (W)	140	139	136	–	–	5	–	67	54	–	52	39	–	–	–	–	–	–	–	23.8	23.5	23.0	–	–	–
Nimonic 105 (W)	–	–	102[a]	–	–	–	–	72.8[b]	60.5[b]	–	44.8	31.6	–	–	–	–	–	–	–	–	–	–	–	–	–
Nimonic 115 (W)	117	–	100	25	23	20	98	77	62	76	55	42	1.0	96	74	57	66	47	34	–	–	–	8.4	8.5	8.6
Rene'41 (W)[e,g]	107	103	97	11	12	14	92	68	50	65	45	29	0.2	67	45	30	44	29	18	24.8	24.4	24.0	8.2	8.3	8.5
Rene'41 (W)[e,g]	136	130	118	11	11.5	14	90	64	40	60	38	24	0.2 1.0	61 –	39 –	22 –	39 70	17 40	4 25	24.8	24.4	24.0	8.2	8.3	8.5
Udimet 700 (W)	120	116	110	23	25	29.5	94	78	64	76	58	43	1.0	–	–	–	–	46	29	24.0	23.5	22.8	8.3	–	8.6
Unitemp 1753 (W)	120	115	110	15	–	15	–	–	–	60	47	34	1.0	–	–	–	52	42	–	24.2[d]	–	23.5[d]	7.8	7.9	8.0
Waspaloy (W)	98	95	90	28	28.3	29	79	60	42	58	40	26.5	1.0	–	–	–	36	25	14	22.5	22.0	21.3	8.6	8.7	8.8
GMR-235 (C)	78	74	60	–	–	–	–	–	–	52	38	25	1.0	50	43	36	39	31	22	23.6	23.3	22.7	8.1	8.2	8.3
IN-100 (C)	120	118	115	6	5.5	5	–	–	–	85	72	59	–	–	–	–	–	–	–	–	–	–	–	–	–
Inco 713C (C)	103	101	97	5	5	5	–	81	72	70	55	41	0.2	36	29	22	28	22	15	27.1	26.5	25.0	8.2	8.3	8.5
Nicrotung (C)	96	94	90	6	4	3	–	–	–	–	65	–	1.0	–	–	–	75	62	50	–	–	–	–	–	–
SM-200 (C)	123	122	121	3.2	3	3	92	90	–	81	73	–	–	–	–	–	–	–	–	–	–	–	–	–	–
SM-302 (C)	56	54	52	8	8.5	9.5	–	–	–	49	–	40	–	–	–	–	–	–	–	–	–	–	8.0	8.1	8.1
SM-322 (C)	51	50	–	6	–	–	61	48	36	49	38	26	–	–	–	–	–	–	–	–	–	–	–	–	–
Inconel X (W)	70	–	60	10	–	20	45[c]	36[c]	–	35	28	18	0.2	–	–	–	32	27	16	21	–	18	8.7	–	9.0
N-155 (W)	36	–	30	31	–	32.5	36[b]	28[b]	22[b]	26	17.5	15	1.0	–	–	–	–	15	13	22.1	–	21.1	9.7	–	9.8
S-816 (W)	40	–	38	25	–	21	43	32.5	25	31.2	23.7	16.5	–	–	–	–	–	–	–	26.2	–	25.8	8.8	–	8.9

Note: W = wrought; C = cast.

(a) 1470 F.
(b) 1350 F.
(c) 1425 F.
(d) Dynamic.
(e) Sol. tr. 2150 F, 2 hr; AC. Aged 1650 F, 4 hr; AC.
(f) Sol. tr. 1950 F, 4 hr; AC. Aged 1400 F, 16 hr; AC.
(g) Modulus of Elasticity E = 32 x 10^6 psi at 70 F.

BATTELLE MEMORIAL INSTITUTE

available on Nimonic 115. IN 100 has gained little commercial acceptance, and little is known of the alloy other than the properties cited.

Extensive experience, on the other hand, has been gained in the use of René 41. The alloy is available as forgings, billets, bar, and sheet from several sources. It has excellent strength properties over the temperature range from 70 to 1500 F. In fact, it was for this temperature range that René 41 was specifically designed. It was not designed to be used at temperatures above 1500 F.

For these reasons, René 41 was selected as the most promising material for high-temperature separable connectors. Table 3 cites the short-time-tensile and the available crrep-rupture properties of René 41. Complete time-deformation curves during creep testing are required in designing connectors for high-temperature use. To obtain specific data for design purposes, a family of complete creep curves at a number of stresses at 1440 F is required. Such curves were not available in the literature. In most creep testing, loads are usually selected to produce rupture in 1000 hours or less. Such loads can result in 0.2 to 0.3 per cent deformation on loading. At lower stress levels where smaller per cent deformation on loading occurs, rupture lives of several thousand hours will result. Such tests are seldom run, and if they are, complete creep data are not reported. Nevertheless, a few complete creep curves for René 41 in the temperature range of interest were uncovered in References (12,13).

Relaxation data on René 41 were not available in the literature.

René 41 is a precipitation-hardenable nickel-base alloy. The material is usually supplied in the solution-annealed condition. Hardening is accomplished by aging the alloy at 1400 or 1650 F. This causes precipitation of a complex nickel-titanium-aluminum phase (called the gamma-prime phase) and produces excellent strength over the temperature range of interest.

René 41 is readily forged and considerable experience has been accumulated by many forge shops in working the alloy. Like most high-strength nickel-base alloys, René 41 work hardens rapidly during machining and is considered difficult to machine. Nevertheless, it is machined by many shops on a production basis.

René 41 is considered a weldable alloy. Nevertheless, as is the case with all high-strength precipitation-hardenable alloys, welding may be somewhat of a problem. Welding in the solution-annealed condition (the low-strength condition) is recommended. After welding, the part should be reannealed and aged to obtain the properties cited. Welding in the aged condition, particularly under conditions of stress, is not recommended. This is true of all precipitation-hardenable nickel-base alloys. In general, it has been found that the greater the aluminum plus titanium content, the higher is the strength and the more difficult are the welding operations. The use of a significantly more weldable material will consequently entail a very appreciable reduction in strength and a sizable weight penalty.

Two specific heat treatments have been developed for René 41: one to develop maximum short-time strength and one to develop maximum long-time creep and rupture strengths. The former treatment involves solution treating at 1950 F for 4 hours, air cooling, and aging at 1400 F for 16 hours. This treatment yields good short-time tensile properties and acceptable 10-hour rupture and creep strengths. The latter treatment, involving solution treating at 2150 F for 2 hours, air cooling, and aging at

1650 F for 4 hours, produces somewhat reduced short-time tensile properties but significantly improved long-time creep and rupture strength. As indicated previously, René 41 should be welded in the solution-treated condition. Recent welding studies have revealed problems in weld metal cracking for material welded after the high-temperature treatment (2150 F). The use of the lower temperature treatment (1950 F) has reportedly eliminated weld-metal-cracking problems. For this reason, a solution-treatment temperature of 1950 F and an aging treatment of 1400 F are recommended. With such a heat treatment, high short-time tensile properties and good 10-hour rupture and creep properties will be obtained. A sacrifice in long-time creep and rupture strength will result. Long-time strength is not a prime requirement for the present application.

René 41 has excellent oxidation resistance over the specified service-temperature range. It is not known to become embrittled in this temperature range. While comparative data on resistance to thermal shock are not available, it is believed that the alloy has comparable or better resistance to thermal shock than the other candidate materials.

Finally, it is not anticipated that René 41 will show a tendency to bonding or self-welding during service. Alloys which contain appreciable amounts of chromium, aluminum, and titanium are exceedingly difficult to bond. Bonding is accomplished only in atmospheres capable of reducing the stable spinel-type oxide on the surface of the alloy and under conditions of high temperature, high stress, and relative metal flow at mating surfaces. Consequently, self-welding of connectors of this alloy is not to be expected. If sticking of the connector is encountered, oxidation of the mating surfaces of the connector should reduce, if not eliminate, the problem. Heating the connector at about 1800 F in an atmosphere containing a low oxygen content should produce a hard, thin oxide layer which is exceedingly difficult to remove. Such an oxide film should prevent self-welding of the connector. If self-bonding persists, the deposition of a very thin layer of titanium or aluminum on the mating surfaces of the connector is recommended. The thin film should be diffused into the connector and oxidized by heating to high temperatures, such as solution treating at 1950 F. This should prevent self-welding.

In summation, René 41 has been selected as the material of construction for high-temperature separable connectors operating from room temperature to 1440 F. Certain other alloys have better creep strength than René 41; however, the combination of properties obtainable in René 41, as well as the availability and experience gained on this alloy, strongly recommends it.

This survey and the recommendations were made with limited knowledge of the tubing material that will be used with the René 41 connector. If the connector is to be welded to the tubing, knowledge of the tubing material is required before the weldability and the compatibility of the connector and the tubing can be ascertained. Welding dissimilar materials is often a major problem. While it is not the purpose herein to select a tubing material, consideration was given to various tubing materials capable of being employed with René 41 connectors. René 41 tubing is not currently commercially available. The high-temperature tubing materials capable of being employed in this application and currently commercially available are Inconel X, Hastelloy X, Inconel 718, and Waspaloy. Inconel X, Hastelloy X, and Inconel 718 are of significantly different composition than René 41. In addition, these alloys have significantly lower strength at the design temperature than René 41, and the heat treatments employed to strengthen these alloys are not compatible with that recommended for René 41. In

comparison, Waspaloy is quite similar in composition to René 41, and has similar physical and mechanical properties. The heat treatment of René 41 is compatible with that of Waspaloy, and welding René 41 connectors to Waspaloy tubing is feasible.

It is therefore suggested that Waspaloy be given full consideration as the tubing material for use with René 41 connectors. Both the tubing and the connector should be in the solution-treated condition for welding. After welding, the assembly must be completely heat treated. The heat treating sequence recommended is as follows:

(1) Solution treat at 1975 F for 4 hours, air cool

(2) Stabilize at 1550 F for 24 hours, air cool

(3) Age at 1400 F for 12 hours, air cool.

This heat treatment is recommended for Waspaloy. The René 41 connectors, when subjected to this heat treatment, will have properties comparable to those reported herein.

Design Properties of René 41

The minimum or steady-state creep rates are determined from the master creep curve of Reference (14), shown in Figure 5. The data of Figure 5 are replotted in Figure 6 for 1440 and 1500 F. The straight dashed lines in Figure 6 are a conservative fit to the data at the two temperatures. The corresponding constants are:

At 1440 F,

$$C_1 = 4.23 \times 10^{-28},$$

$$n = 4.97.$$

At 1500 F,

$$C_1 = 1.30 \times 10^{-26},$$

$$n = 4.82.$$

A rapid method for determining the constants C_1 and n from creep data, using the creep law $\dot{\epsilon} = C_1\sigma^n$, is as follows:

Determine the strain rates $\dot{\epsilon}_1$ and $\dot{\epsilon}_2$ for the stresses σ_1 and σ_2, respectively. From the steady-state creep law, $\dot{\epsilon}_1/\dot{\epsilon}_2 = (\sigma_1/\sigma_2)^n$, where n is the only unknown, and is easily solved. After calculating n, the constant C_1 can be determined from $\dot{\epsilon}_1 = C_1\sigma_1^n$.

The constants C_2 and m for the intercept stress were obtained from the test data and plotted curves of Reference (13). Since the intercept data of Reference (13) are not very consistent, the following constants are considered only approximate in magnitude. This is one reason for the recommendation that creep data be generated for René 41 at 1440 F.

At 1440 F,

$C_2 = 1.25 \times 10^{-8}$,

$m = 1.00$.

At 1500 F,

$C_2 = 3.93 \times 10^{-11}$,

$m = 1.57$.

The design data for René 41 at 1440 F and 1500 F are plotted in Figure 7 for various stress levels.

Other design properties of René 41 are obtained from Tables 2 and 3.

The yield strength $\sigma_y = 120{,}000$ psi at 70 F,

$\sigma_y = 103{,}000$ psi at 1440 F,

$\sigma_y = 97{,}000$ psi at 1500 F.

The modulus of elasticity $E_R = 32.0 \times 10^6$ psi at 70 F,

$E_T = 24.4 \times 10^6$ psi at 1440 F,

$E_T = 24.0 \times 10^6$ psi at 1500 F.

The mean coefficient of thermal expansion $\alpha = 8.3 \times 10^{-6}$ in/in/°F at 1440 F,

$\alpha = 8.5 \times 10^{-6}$ in/in/°F at 1500 F.

DESIGN PROCEDURE

Basis for Design Procedure

The design procedure considers only the elastic and creep behavior of the bolts and flange assembly. Secondary effects such as flange rotation due to internal pressure, creep of the gasket, creep of the threads, creep bending of the bolt, and dynamic creep are not included in the design procedure, but are discussed in Appendix C. The design factor of safety is intended to account for these secondary effects in addition to the scatter in material properties.

The gasket (seal) design for mechanical fittings is not included in the design procedure, but is discussed in Reference (11), where it was concluded that plastic yielding of seal surfaces is desirable for effective sealing. An initial seating stress as high as 2.75 times the yield strength of the metal gasket material was considered necessary to achieve the desired degree of yielding in order to keep the leakage rate of helium below the tolerable level[11].

It is assumed that the bolts are flexible compared to the gasket in order that the application of internal pressure results in negligible bolt-load changes. It is not necessary that the gasket be the only load path through the assembly.

The design procedure is intended primarily as a method for calculating relaxation of the connector assembly, and does not include a failure analysis of the component parts. It is assumed that the material possesses sufficient ductility to withstand the progressive deformation incurred if the connector assembly is retightened after each cycle. Various methods of analysis available for predicting the tube strains are discussed in Appendix D. These methods are intended for the tube design at locations sufficiently removed from discontinuities such as the connector assembly.

The detailed design procedure for bolted-flanged and threaded connectors is described step-by-step for the purpose of obtaining a curve of leakage pressure versus time (or a time to leakage for a specific value of the design pressure). The effects of external loads, temperature differentials, and retightening, and the use of relaxation data are discussed separately from the basic design procedure.

The equations used in the design procedure are derived in Appendix B.

Bolted-Flanged Connectors

The basic design procedure for a bolted-flanged connector consists of nine specific steps in order to arrive at a curve of leakage pressure versus time. Figure 8 shows a typical flange geometry.

(1) Design Conditions

Establish the design temperature, design pressure, nominal connector diameter, tube geometry, life requirements, and temperature differentials.

(2) Material Properties

Determine the yield strength σ_y and the modulus of elasticity E at both room temperature and the design temperature, and the coefficient of thermal expansion α at the design temperature.

From a family of creep curves at the design temperature, determine the constants C_1, C_2, m, and n to fit the following equation:

$$\epsilon = \epsilon_e + \left(C_2 \sigma_o^{\ m} + C_1 \sigma_o^{\ n} \right) t \ . \qquad (1)$$

The creep constants should be selected to give the best fit to the experimental data in the range of stress levels expected in the design*.

(3) ASME Code Design

The design procedure can be applied to any arbitrary design. However, it is desirable to use the ASME Boiler and Pressure Vessel Code[1] for the initial static design in order to establish a balanced design. Also, the Code-rated flange can subsequently be rated on a life basis for comparison.

Using the rules of the ASME Code[1], establish either a loose-type or integral-type flange geometry for an appropriate value of internal pressure. This pressure, of course, should be at least as high as the design pressure multiplied by the ratio of the cold-to-hot modulus of elasticity, and multiplied by the design factor of safety. The initial gasket seating load will be dependent on the type seal used and the maximum permissible leakage rate, and need not follow the rules of Reference (1). The allowable Code stress is assumed to equal two-thirds of the room-temperature yield strength in order to avoid yielding of the assembly during the bolt-up operation.

The ASME Code will establish a static design at room temperature. The initial bolt load and bolt stress at room temperature are designated as P_{BR} and σ_{BR}, respectively.

(4) Flexibility Equations

Determine the bolt flexibility F_B (bolt deflection due to a unit bolt load):

$$F_B = \frac{L_B}{A_B E_T} \ , \qquad (2)$$

*Further details on the creep constants and the intercept stress reduction are given on pages 6, 15, and B-3.

where

L_B = effective length of the bolt, usually taken as the total length between the nut bearing surfaces plus one nominal bolt diameter,

A_B = total bolt area based on root diameter.

Determine the flange flexibility F_F (total deflection of two flanges at the bolt circle due to a unit bolt load).

For a loose-type flange,

$$F_F = \frac{3.82\, e^2}{E_T h^3 \ln d_F/c_F} \quad . \tag{3}$$

For an integral-type flange,

$$F_F = \frac{1.29\, Ve^2}{L\sqrt{c_F}\,(d_T - c_T)^{5/2}\, E_T} \quad . \tag{4}*$$

(5) Creep Equations

Calculate the rate of creep deflection of the bolts K_B and the rate of creep deflection of the two flanges at the bolt circle, K_F:

$$K_B = \frac{C_1 P_t^{\,n} L_B}{A_B^{\,n}} \quad , \tag{5}$$

and

$$K_F = \frac{4\sigma_{Ft}^{\,n} C_1 e c_F}{h} \quad , \tag{6}$$

where

$$\sigma_{Ft} = \left(\frac{h}{2c_F}\right)^{\frac{1}{n}} \left(\frac{P_t e}{2\pi}\right) \left[\frac{\left(2^{1+\frac{1}{n}}\right)\left(1-\frac{1}{n}\right)\left(2+\frac{1}{n}\right)}{\left(d_F^{\,1-\frac{1}{n}} - c_F^{\,1-\frac{1}{n}}\right) h^{2+\frac{1}{n}}}\right]$$

Equation (6) applies only to a loose-type flange. The creep rate of an integral-type flange is assumed equal to that of the loose-type flange, provided the maximum design stresses according to Reference (1) are equal. The procedure for an integral-type flange is to calculate the maximum design stress by Reference (1). Then determine the thickness of a loose-type flange with the same flange inner and outer radii, moment arm, and maximum design stress as the integral-type flange; this results in an equivalent strength loose-type flange. Using the loose-type flange geometry, calculate the creep rate from Equation (6), assuming this to be the creep rate of the integral-type flange.

*The terms V and L in Equation (4) conform to the nomenclature of Reference (1).

(6) Flexibility and Creep Ratios

Calculate the life factor R for the purpose of conveniently evaluating a flange geometry on a life basis:

$$R = \frac{1 + r_F}{1 + r_K} \quad , \tag{7}$$

where

r_F = flexibility ratio = F_F/F_B ,

r_K = creep ratio = K_F/K_B .

Equations (5) and (6) should be calculated in terms of the bolt load P_t, in order that the creep ratio r_K be calculable.

(7) Intercept Stress Reduction

Calculate the bolt stress, σ_{BT}. The initial room-temperature bolt stress σ_{BR} is reduced to a new value σ_{BT} at the design temperature due to the change in modulus of elasticity:

$$\sigma_{BT} = \sigma_{BR}\left(\frac{E_T}{E_R}\right) . \tag{8}$$

Calculate a further reduction in bolt stress from σ_{BT} to a value σ_o due to the effects of primary creep:

$$\sigma_o = \sigma_{BT} - \frac{E_T C_2 \sigma_o^{\,m}}{R} \quad . \tag{9}$$

Equation (9) is conveniently solved for σ_o by trial and error. The bolt stress σ_o or corresponding bolt load P_o represents the actual starting point in the life calculations.

(8) Bolt Relaxation

Calculate the time t required for the bolt stress to relax from an initial value σ_o to a new value σ_t:

$$t = \frac{R}{C_1 E_T (n-1)} \left[\frac{1 - \left(\frac{\sigma_t}{\sigma_o}\right)^{n-1}}{\sigma_t^{\,n-1}}\right] \quad . \tag{10}$$

(9) Leakage Pressure

Solve Equation (10) successively in order to obtain a curve of residual bolt stress σ_t or load P_t versus time. Convert these results to an allowable leakage pressure versus time curve by the successive solution of Equation (11):

$$P_t' = P_p + P_G \quad , \tag{11}$$

where

$P_t' = \frac{P_t}{F.S.}$,

P_p = bolt load due to pressure = $\pi p g^2$,

P_G = residual gasket load (or load across flange face) required to prevent excessive leakage (the determination of this load is not included in this report).

In Equation (11), P_t' is established directly from the P_t versus t curve by applying a suitable factor of safety to the load rather than the time scale. The value P_G is dependent on the type of gasket used, and may or may not be a function of the internal pressure p.

Threaded Connectors

The design procedure for threaded connectors commences with Step 1 (design conditions) and Step 2 (material properties) of the bolted-flanged connector design procedure. Six additional steps are then required for the threaded connector in order to obtain a leakage pressure versus time curve.

Reference (15) can be used for the static design of a threaded connector. The nomenclature for the parts of the threaded connector is based on the functional analogy to the parts of the bolted-flanged connector and is not to be taken as a literal description of the parts. A threaded connector model is shown in Figure 9. The nut is considered the "bolt" member of the analysis, and contributes both axial and bending deformations. The flange and union members in Figure 9 are considered the "flange" member of the analysis with axial deformation only.

(1) "Bolt" Flexibility

Calculate the "bolt" flexibility F_B, which represents the axial flexibility of the nut and has the same form as Equation (2):

$$F_B = \frac{L_B}{A_B E_T} \quad , \tag{12}$$

where L_B and A_B are the effective nut length and area, respectively.

Calculate the bending flexibility of the "bolt" F_B' by using the development on pages 194-197 of Reference (15) for inwardly projecting flanges (see Figure 10):

$$F_B' = e^2 \left(\frac{\theta}{M}\right) , \tag{13}$$

where

$$\frac{\theta}{M} = \frac{3(1-\nu^2)}{\pi d_T \beta (d_T - c_T)^3 E_T \left[\frac{(1-\nu^2)}{2\beta d_T}\left(\frac{h}{d_T - c_T}\right)^3 \ell n \frac{d_T}{c_F} + 1 + \frac{\beta h}{2}\right]}$$

and

$$\beta = \sqrt[4]{\frac{3(1-\nu^2)}{d_T^2 (d_T - c_T)^2}} \quad .$$

(2) "Flange" Flexibility

Calculate the axial flexibility of the "flange", F_F:

$$F_F = \frac{L_F}{A_F E_T} \quad . \tag{14}$$

The effective length L_F can be considered equal to L_B in Equation (12). A_F is the cross-sectional area of the "flange".

(3) "Bolt" Creep

Calculate the axial creep rate of the "bolt", K_B:

$$K_B = \frac{C_1 P_t^{\,n} L_B}{A_B^{\,n}} \quad . \tag{15}$$

Calculate the bending creep rate of the "bolt", K_B', in a manner similar to an integral-type flange*, except that the maximum design stress is determined from Reference (15) for an inwardly projecting flange.

The longitudinal hub stress S_H, radial ring stress S_R, and tangential ring stress S_T, respectively, are

$$S_H = \frac{3M}{\pi d_T (d_T - c_T)^2 \left[\frac{(1-\nu^2)}{2\beta d_T}\left(\frac{h}{d_T - c_T}\right)^3 \ln \frac{d_T}{c_F} + 1 + \frac{\beta h}{2}\right]} \quad ,$$

$$S_R = \frac{3(1 + \frac{\beta h}{2})M}{\pi d_T h^2 \left[\frac{(1-\nu^2)}{2\beta d_T}\left(\frac{h}{d_T - c_T}\right)^3 \ln \frac{d_T}{c_F} + 1 + \frac{\beta h}{2}\right]} \quad , \tag{16}$$

*See procedure on page 19 for integral-type flanges.

$$S_T = \frac{3(1-\nu^2)hM}{2\pi d_T c_F (d_T - c_T)^3 \beta \left[\frac{(1-\nu 2)}{2\beta d_T} \left(\frac{h}{d_T - c_T}\right)^3 \ln\frac{d_T}{c_F} + 1 + \frac{\beta h}{2}\right]} ,$$

where $\beta = \sqrt[4]{\frac{3(1-\nu^2)}{d_T{}^2 (d_T - c_T)^2}}$.

The maximum stresses from Equations (16) should be combined according to the method of Reference (1). For a threaded connector, Equation (6) herein should be used with a constant of two rather than four because there is one rather than two flange members.

(4) "Flange" Creep

Calculate the axial creep of the "flange", K_F, which has the same form as Equation (15):

$$K_F = \frac{C_1 P_t{}^n L_F}{A_F{}^n} . \qquad (17)$$

(5) Flexibility and Creep Ratios

Calculate the life factor R:

$$R = \frac{1 + r_F + r_F'}{1 + r_K + r_K'} , \qquad (18)$$

where

$$r_F = F_F/F_B \ , \ r_F' = F_B'/F_B \ ,$$

$$r_K = K_F/K_B \ , \ r_K' = K_B'/K_B \ .$$

(6) Nut Relaxation

Determine the relaxation of the nut from Equation (10), but using the life factor R from Equation (18). Use Equation (11) to calculate the leakage pressure versus time.

External Loads

Determine the effect of external loads on the leakage pressure by revising Equation (11) to read:

$$P_t' = P_p + P_G + P_A + P_M \quad , \tag{19}$$

where P_A and P_M include the effects of external thrusts and moments, respectively:

$$P_A = \pi p K_A c_T^2 \quad ,$$
$$P_M = \frac{\pi p K_M c_T^2 (d_T^2 + c_T^2)}{2 d_T g} \tag{20}$$

Solve Equation (19) successively in order to obtain a leakage pressure versus time curve.

The constants K_A and K_M are used to define the magnitude of the stress due to tube thrusts (σ_A) and moments (σ_M), respectively, in terms of the axial tube stress (σ_T) due to internal pressure:

$$K_A = \frac{\sigma_A}{\sigma_T} \quad , \quad K_M = \frac{\sigma_M}{\sigma_T} \quad ,$$

where

$$\sigma_T = \frac{p c_T^2}{(d_T^2 - c_T^2)} \quad .$$

Temperature Differentials

The analysis of temperature differentials is limited herein to the case of components at uniform temperatures, but at a different average temperature from another component of the assembly. In one case, the bolt is assumed to be at a different average temperature than the flange and tube assembly, probably the more critical case. In the other case, the flange and bolt assembly is assumed to be at a different average temperature than the tube. The change in material properties with temperature change is neglected in the thermal calculations. It is also assumed that the temperature differentials are of a short-time nature, occurring almost instantaneously for the purpose of analysis. A more refined analysis would be required for temperature differentials varying considerably with time.

Bolt-Flange Differential

Letting a positive value of ΔT represent the flange at a higher average temperature than the bolt, calculate the change in bolt stress $\Delta\sigma_B$:

$$\Delta\sigma_B = \frac{\alpha(\Delta T) E_T}{1 + r_F} \quad . \tag{21}$$

For a threaded connector, the change in "bolt" (nut) stress is

$$\Delta\sigma_B = \frac{\alpha(\Delta T)\, E_T}{1 + r_F + r_F'} \quad . \tag{22}$$

The change in bolt or nut load in Equations (21) and (22) should be evaluated in a different manner, depending upon the nature of the differential. A positive temperature differential at the start of the cycle would lead to an increase in the bolt load. This increase should be used to guard against overstressing of the bolt (or other connector components), and neglected for short-time differentials in the relaxation analysis. If a negative temperature differential should occur near the end of the operating cycle, the reduction in bolt load should be added to Equation (11) to determine a reduced leakage pressure:

$$P_t' = P_p + P_G + P_T \quad , \tag{23}$$

where $P_T = \Delta\sigma_B A_B$ (bolt-load change due to temperature differential).

Flange-Tube Differential

The analysis by Dudley[16] or an extension of the equations presented by Rodabaugh in discussion of Reference (17) can be used to evaluate bolt-load changes due to the tube and flange assembly being at different average temperatures. The method of Rodabaugh[17] is preferred, since it is consistent with the basic equations of the ASME Code[1]. At the start of the operating cycle the tube will possibly be hotter than the remaining assembly, thus causing a reduction in the bolt load. The opposite effect may occur upon cooling down the assembly. An increase in the bolt load should be used to guard against overstressing the connector assembly, whereas a decrease in the bolt load should be used in Equation (23).

Retightening

If the assembly is not retightened between operating cycles, a continuous operating cycle is assumed, consisting of the total time of the individual cycles. This procedure is consistent with the assumption that creep strains are irreversible in nature.

In the event that retightening is contemplated, each cycle is reanalyzed according to the creep design procedure (not repeating static design) as though it were the first cycle. This is a conservative approach because the flange life will probably improve on subsequent cycles to the extent that the primary creep strains are nonrecurring, as evidenced by the British Flange Tests[9].

Relaxation Data

The design procedure is based on the assumption that only creep data are available. Of course, relaxation data are preferred. Relaxation data should be available as a

family of curves, starting from various initial stress levels, sufficient to cover the range of initial stress levels expected in the design.

Since the relaxation test is usually run with no elastic follow-up (R = 1), the time required for a connector assembly bolt or nut stress to relax from an initial stress σ_o to a final value σ_t is obtained directly from the relaxation test data, multiplied by the life factor R determined from Equation (7) or (18). If the relaxation tests are run with elastic follow-up, the relaxation time is determined by multiplying the test data (time) by the ratio of the life factor R of the connector to that of the test assembly. Interpolation of the test data may be required for specific values of the initial stress σ_o not available in the test data. The use of a direct ratio for various values of the life factor is based on the assumption that the life factor is a constant in the analysis. Baumann[2] justifies this approach, regardless of the creep law observed by the material.

The direct use of relaxation data results in a residual stress versus time curve, similar to that yielded by Equation (10). In generating relaxation data, it would be desirable to run at least one test with sufficient elastic follow-up to simulate the life factor of a connector assembly.

Redesign Considerations

The designer may find that the calculated connector life for a particular design pressure is less than the required design life. If the temperature and material have already been fixed, the only changes that can be made in order to obtain an improved life are geometry changes. Ordinarily, the connector inner diameter, bolt geometry, and gasket geometry will be kept constant during a redesign. Therefore, the logical changes to make if the life factor R in Equation (10) is to be improved are changes in the flange thickness, flange width, and moment arm.

Changes in the moment arm e can have an appreciable effect on the life factor R. Of course, an increase in the moment arm will have to be compensated for by changes in the flange width and/or thickness (or hub geometry for an integral-type flange) in order that the flange stresses be maintained at an acceptable level. It is recommended that improvements in the connector life be made by simultaneous changes in the moment arm for flange bending, the flange width, and the flange thickness. Effects of changes in the length of the bolt L_B (perhaps with the use of a rigid bolt collar) should also be investigated.

If the desired connector life is not attained by the changes described above, the next logical step would be to redesign the bolt geometry and gasket geometry in order to allow for greater percentage reductions in the initial bolt load before leakage occurs.

DISCUSSION OF SAMPLE CALCULATIONS

The sample calculations are presented in order to adequately demonstrate the design procedure, and not to arrive at optimum design connectors. An optimum design can be determined only after calculating a wide range of connector geometries, thus enabling the selection of a minimum-weight design for a given combination of design (leakage) pressure and life.

The loose-type and integral-type flange geometries of Figures 11 and 12, respectively, have nearly the same initial stress σ_o, and the life factor R differs by only 10 per cent. Therefore, the results in Figures 13 and 14 for the loose-type flange very nearly apply for the integral-type flange. The loose-type flange is heavier. This will not always be the case since the loose-type flange can frequently have a much higher flexibility than the equivalent integral-type flange.

The factor of safety used in Figure 13, together with the intercept stress reduction and the bolt load reduction due to change in elastic modulus, leads to a maximum design pressure of 2980 psi in Figure 14, assuming no external loads or temperature differentials. It is shown that a temperature difference between the bolt and flange assembly of -100 F severely affects the leakage pressure and establishes a limiting life of 38 hours. The curves of Figure 14 indicate that, up to approximately 0.5 hour, there is negligible change in the leakage pressure. This would infer that, for accumulated life cycles totaling 0.5 hour or less, retightening after each cycle would not be very beneficial.

René 41 at 1500 F does not exhibit a great deal of primary creep, as shown by the relative insensitivity of the initial stress σ_o to the life factor R in Figure 15. For some materials, the effect of the life factor on the reduced intercept stress would be a strong influence in choosing an optimum design. The life factor R is a convenient measure of the relative merits of various designs with the same initial bolt stress because it is essentially a geometry-dependent constant in the relaxation equation, all other constants in Equation (10) being a function only of the material and temperature.

It is usually considered desirable to preload the bolt or nut as high as possible without yielding any portions of the connector assembly. The high preload is intended to delay the relaxation of stress or load. Various values of the initial bolt stress were used in the relaxation equation (27). The results in Figure 16 indicate that, for design lives over 1-2 hours, there is very little advantage gained by higher prestressing. In fact, the initial prestress σ_o of 45,000 psi would be more desirable for longer lives since it will provide greater safety against yielding. The initial stress of 90,000 psi at 1500 F for René 41 would be difficult to obtain because of the intercept stress reduction, the elastic modulus change, and the limitation imposed on the room-temperature bolt preload to avoid yielding.

Results of the threaded-connector geometry of Figure 17 are shown in Figure 18. The geometry of Figure 17 does not represent a well-balanced design. As a result, the axial nut stress σ_{BR} is limited to 40,000 psi (room-temperature prestress) to avoid overstressing the inwardly projecting flange. The low prestress results in the relatively slow relaxation of the nut load shown in Figure 18.

It is quite possible that the optimum static design will also provide a good design for relaxation, depending upon the material and design temperature. However, for some combinations of material and temperature, the sound static design approach may not suffice because of the importance of the interaction of bolt and flange creep and flexibility ratios. For a static design, the integral-type bolted flange is usually lighter than the loose-type flange. This may not be true for relaxation design. In some cases, loose-type flanges offer advantages in the way of increased flexibility and the ability to better withstand certain types of temperature differentials.

REFERENCES

(1) ASME Boiler and Pressure Vessel Code, Section VIII, "Rules for Construction of Unfired Pressure Vessels", New York (1962).

(2) Baumann, K., "Some Considerations Affecting Future Developments of the Steam Cycle", Engineering, 130, 597-599, 661-664, 723-727 (1930).

(3) Bailey, R. W., "The Utilization of Creep Test Data in Engineering Design", Proceedings of the Institution of Mechanical Engineers, 131, 131-349 (1935).

(4) Bailey, R. W., "Flanged Pipe Joints for High Pressures and Temperatures", Engineering, 144, 364-365, 419-421, 490-492, 538-539, 615-617, 674-676 (1937).

(5) Waters, E. O., "Analysis of Bolted Joints at High Temperature", Transactions of the ASME, 60, 83-86 (1938).

(6) Marin, J., Mechanical Properties of Materials and Design, McGraw-Hill Book Co., Inc., New York (1942).

(7) Finnie, I., and Heller, W. R., Creep of Engineering Materials, McGraw-Hill Book Co., Inc., New York (1959).

(8) Gough, H. J., "First Report of the Pipe Flanges Research Committee", Proceedings of the Institution of Mechanical Engineers, 132, 201-340 (1936).

(9) Tapsell, H. J., "Second Report of the Pipe Flanges Research Committee", Proceedings of the Institution of Mechanical Engineers, 141, 433-471 (1939).

(10) Johnson, A. E., "Pipe Flanges Research Committee – Third Report", Proceedings of the Institution of Mechanical Engineers, 168, 423-463 (1954).

(11) Rathbun, F. O., Jr., "Design Criteria for Zero-Leakage Connectors for Launch Vehicles, Vol 3, Sealing Action at the Seal Interface", General Electric Advanced Technology Laboratories Report No. 63GL43 (March 15, 1963).

(12) Aarnes, M. N., and Tuttle, M. M., "Presentation of Creep Data for Design Purpose", ASD Technical Report 61-216 (June, 1961).

(13) Gluck, J. V., and Freeman, J. W., "Effect of Creep – Exposure on Mechanical Properties of René 41", ASD Technical Report 61-73 (August, 1961).

(14) Sachs, G., and Pray, R. F., "Air Weapons Materials Application Handbook – Metals and Alloys", ARDC Report TR 59-66.

(15) Rodabaugh, E. C., et al., "Development of Mechanical Fittings", Edwards Air Force Base Report No. RTD-TDR-63-1115 (December, 1963).

(16) Dudley, W. M., "Deflection of Heat Exchanger Flanged Joints as Affected by Barreling and Warping", Transactions of the ASME, Series B, 83, 460-466 (November, 1961).

(17) Wesstrom, D. B., and Bergh, S. E., "Effect of Internal Pressure on Stresses and Strains in Bolted-Flanged Connections", Transactions of the ASME, 73, 121-136 (1951).

(18) Timoshenko, S., "Strength of Materials – Part II", D. Van Nostrand Co., Inc. (1956).

(19) Marin, J., "Stresses and Deformations in Pipe Flanges Subjected to Creep at High Temperatures", Journal of the Franklin Institute, 226, 645-657 (1938).

(20) MacCullough, G. H., "An Experimental and Analytical Investigation of Creep in Bending", Transactions of the ASME, Journal of Applied Mechanics, 55, 55-60 (1933).

(21) Tapsell, H. J., and Johnson, A. E., "An Investigation of the Nature of Creep Under Stresses Produced by Pure Flexure", Journal of the Institute for Metals, 57 (2), 121-140 (1935).

(22) Davis, E. A., "Creep of Metals at High Temperature in Bending", Transactions of the ASME, Journal of Applied Mechanics, 60, A-29-A-31 (March, 1938).

(23) Findley, W. N., and Poczatek, J. J., "Prediction of Creep – Deflection and Stress Distribution in Beams From Creep in Tension", Transactions of the ASME, 77 (1955).

(24) Hult, J., "Mechanics of a Beam Subject to Primary Creep", Transactions of Chalmers University of Technology, Gothenburg, Sweden (256) (1962).

(25) Voorhees, H. R., Freeman, J. W., and Herzog, J. A., "New Investigations Relating to Stress Concentrations Under Creep Conditions", Transactions of the ASME, Journal of Basic Engineering, 84, 207-213 (June, 1962).

(26) Lazan, B. J., "Dynamic Creep and Rupture Properties of Temperature Resistant Materials Under Tensile Fatigue Stress", ASTM Proceedings, 49, 757-787 (1949).

(27) Vitovec, F. H., and Lazan, B. J., "Fatigue, Creep, and Rupture Properties of Heat Resistant Materials", WADC Technical Report 56-181, ASTIA AD 97240 (August, 1956).

(28) Langenecker, B., "Acoustic Radiation Damage in Materials", Presented at Leak-Tight Separable Fluid Connector Design Conference at Huntsville, Alabama (March 24-25, 1964).

(29) Finnie, I., "Steady-State Creep of a Thick-Walled Cylinder Under Combined Axial Load and Internal Pressure", ASME Paper No. 59-A-57.

(30) Finnie, I., "An Experimental Study of Multiaxial Creep in Tubes", 1963 Joint International Conference on Creep.

(31) Rimrott, F. P. J., Mills, E. J., and Marin, J., "Prediction of Creep Failure Time for Pressure Vessels", Transactions of the ASME, Journal of Applied Mechanics, 27, 303-308 (June, 1960).

(32) Davis, E. A., "Creep Rupture Tests for Design of High-Pressure Steam Equipment", Transactions of the ASME, Journal of Basic Engineering, 82, 453-461 (June, 1960).

(33) Rattinger, I., and Padlog, J., "Design Implications of Creep in Pressurized Cylindrical Shells", Aerospace Engineering, 20, 95-108 (March, 1961).

(34) Coffin, L. F., Jr., Shepler, P. R., and Cherniak, G. S., "Primary Creep in the Design of Internal-Pressure Vessels", Transactions of the ASME, 71, 229-241 (1949).

LMC:ECR:DBR:TMT/all

APPENDIX A

SAMPLE CALCULATIONS

APPENDIX A

SAMPLE CALCULATIONS

The sample calculations are all performed on René 41 at 1500 F. The following design values apply to René 41 at room temperature and at 1500 F*.

The yield strength:

$$\sigma_y = 120,000 \text{ psi at } 70 \text{ F},$$

$$\sigma_y = 97,000 \text{ psi at } 1500 \text{ F}.$$

The modulus of elasticity:

$$E_R = 32.0 \times 10^6 \text{ psi at } 70 \text{ F},$$

$$E_T = 24.0 \times 10^6 \text{ psi at } 1500 \text{ F}.$$

The mean coefficient of thermal expansion $\alpha = 8.5 \times 10^{-6}$ in/in/°F at 1500 F.

The creep and intercept constants at 1500 F are:

$$C_1 = 1.30 \times 10^{-26}, \qquad C_2 = 3.93 \times 10^{-11},$$

$$n = 4.82, \qquad m = 1.57.$$

The ASME Code calculations are based on an internal pressure of 10,000 psi. This corresponds to a reduced value of the design pressure equal to 10,000 (E_T/E_R) (1/F.S.) = 3750 psi for a factor of safety equal to two. Therefore, the maximum possible value of the design pressure is 3750 psi, and will be further reduced due to the effects of primary creep.

Loose-Type Bolted Flange

ASME Code Design**

The allowable stress for use in Reference (1) equals 2/3 (120,000) = 80,000 psi. The geometry is shown in Figure 11.

The tube thickness can be determined from other considerations, such as discussed in Appendix D, to equal 0.210 in.

For the purpose of the bolt design, assume that a residual gasket stress of 3P (P = 10,000 psi, the ASME Code design pressure) is required to maintain the gasket

*Material properties for René 41 are given on pages 15-16.
**Use the nomenclature of the ASME Code[1].

seal. Also, assume that the gasket plating material has a yield strength of 10,000 psi and that it requires a gasket stress of three times the yield strength (y = 60,000 psi) to seat the metallic gasket. For a gasket width 2b = 0.125 in. (assume full width is effective),

$$H_P = 2b \times 3.14G \times 3P = 45,900 \text{ lb},$$

$$H = 0.785\, G^2P = 119,000 \text{ lb},$$

$$W_{m1} = H + H_P = 164,900 \text{ lb},$$

$$W_{m2} = 3.14bGy = 45,900 \text{ lb}.$$

The design bolt load W = 164,900 lb.

The required bolt area is

$$A_{m1} = \frac{164,900}{80,000} = 2.06 \text{ in}^2.$$

Use 10-9/16-in.-diameter bolts with a total root area equal to 1.89 in.^{2}. The bolt stress is

$$S_a = \frac{164,900}{1.89} = 87,300 \text{ psi}.$$

For the flange design,

$$h_G = h_T = 0.663 \text{ in.}, \quad h_D = 0.813 \text{ in.},$$

$$H_D = 0.785\, B^2P = 102,000 \text{ lb},$$

$$H = 0.785\, G^2P = 119,000 \text{ lb},$$

$$H_G = W - H = 45,900 \text{ lb},$$

$$H_T = H - H_D = 17,000 \text{ lb},$$

$$M_D = H_D h_D = 82,800 \text{ lb},$$

$$M_T = H_T h_T = 11,300 \text{ lb},$$

$$M_G = H_G h_G = 30,500 \text{ lb},$$

$$M_o = M_D + M_T + M_G = 124,600 \text{ in-lb},$$

$$S_T = 80,000 \text{ psi},$$

$$K = A/B = 1.90.$$

From Figure UA-51.1 of Reference (1), Y = 3.3.

Then,

$$t = \sqrt{\frac{Y\, M_o}{B\, S_T}} = 1.20 \text{ in.}$$

Flexibility and Creep

From the equations on pages 18-20,

$$F_B = 1.78/E_T \quad , \quad F_F = 1.51/E_T,$$

$$K_B = 0.157 C_1 P_t^{4.82},$$

$$\sigma_{Ft} = 0.215\, P_t,$$

$$K_F = 2.405 \times 10^{-3} C_1 P_t^{4.82},$$

$$r_F = 0.849 \quad , \quad r_K = 0.0153,$$

$$R = 1.82.$$

Bolt Relaxation

From Equations (8) and (9),

$$\sigma_{BT} = 87,300 \left(\frac{24 \times 10^6}{32 \times 10^6} \right) = 65,400 \text{ psi},$$

$$\sigma_o = \sigma_{BT} - \frac{E_T C_2 \sigma_o^m}{R} \quad . \tag{24}$$

Solving Equation (24) by trial and error, $\sigma_o = 52,100$ psi. It is convenient to solve Equation (24) for various values of R in order to construct Figure 15, thus saving considerable calculating time when optimizing the flange geometry. For a rigid flange (R = 1), σ_o would equal 46,000 psi.

From Equation (10), the bolt relaxation equation becomes

$$t = 1.53 \times 10^{18} \left[\frac{\left(\frac{\sigma_t}{\sigma_o} \right)^{n-1}}{\sigma_t^{\,n-1}} \right] \quad . \tag{25}$$

With $\sigma_o = 52,100$ psi, the successive solution of Equation (25) results in the residual bolt-load curve of Figure 13.

Leakage Pressure

In order to convert residual bolt load to leakage pressure assume a factor of safety F.S. = 2.0 on the residual load, establishing the design curve of Figure 13. For example, if it is assumed that leakage will occur when the gasket pressure reaches a value of 3p, Equation (11) becomes

$$P_t' = \pi\, pg^2 + 3pA_G. \tag{26}$$

The solution of Equation (26) for various values of the internal pressure p results in the leakage pressure versus time curve ($K_A = K_M = 0$, $\Delta T = 0$) of Figure 14. For example, at p = 2000, P_t' = 33,000 lb. The time t from Figure 13 for 33,000 lb is 4.9 hours.

Effect of Initial Stress

The relaxation equation for the geometry of Figure 11 is

$$t = 1.53 \times 10^{18} \left[\frac{1 - \left(\frac{\sigma_t}{\sigma_o}\right)^{n-1}}{\sigma_t^{\,n-1}} \right] . \tag{27}$$

The effect of varying the bolt stress σ_o in Equation (27) is shown in Figure 16.

Integral-Type Bolted Flange

ASME Code Design*

An integral-type flange was designed in accordance with Reference (1). The gasket geometry, moment arm, outer flange radius, tube geometry, and design bolt load are the same as for the loose-type flange of Figure 11. The integral-type flange geometry is shown in Figure 12:

$$h_T = 0.868 \text{ in.},\ h_G = 0.663 \text{ in.},\ h_D = 0.863 \text{ in.}$$

From page A-2,

$$W = 164,900 \text{ lb},$$

$$H = 0.785\, G^2P = 119,000 \text{ lb},$$

$$H_D = 0.785\, B^2P = 74,500 \text{ lb},$$

$$H_G = W - H = 45,900 \text{ lb},$$

$$H_T = H - H_D = 44,500 \text{ lb},$$

*Use the nomenclature of the ASME Code(1).

$$M_D = H_D h_D = 64,200 \text{ lb},$$

$$M_T = H_T h_T = 38,600 \text{ lb},$$

$$M_G = H_G h_G = 30,500 \text{ lb},$$

$$M_o = M_D + M_T + M_G = 133,300 \text{ in-lb}.$$

Using an allowable stress of 80,000 psi and a design moment of 133,300 in-lb, the thickness of an integral-type flange is calculated from Reference (1) to be 0.95 in.

Flexibility and Creep

From Equations (2) and (5),

$$F_B = 1.35/E_T,$$

$$K_B = 0.118 C_1 P_t^{4.82}.$$

Since the flange design stress of 80,000 psi is the same as that of the equivalent loose-type flange, the flange creep rate is assumed to equal that of the loose-type flange:

$$K_F = 2.405 \times 10^{-3} C_1 P_t^{4.82}.$$

The flexibility of the integral-type flange from Equation (4) is

$$F_F = 1.43/E_T.$$

Then

$$r_F = 1.06, \quad r_K = 0.0204,$$

$$R = 2.02.$$

Bolt Relaxation

From Figure 15, $\sigma_o = 52,900$ psi. The bolt relaxation equation becomes

$$t = 1.69 \times 10^{18} \left[\frac{1 - \left(\frac{\sigma_t}{\sigma_o} \right)^{n-1}}{\sigma_t^{\,n-1}} \right]. \qquad (28)$$

Equation (28) does not yield results significantly different from Equation (25) for a loose-type flange.

Threaded Connector

Figure 17 shows a threaded-connector geometry, which represents an arbitrary set of dimensions rather than an optimum static design. The design procedure is used to

calculate the design life of the geometry of Figure 17, based on René 41 at 1500 F. Figure 9 is a guide for the proper dimensions to use in the analysis.

Bolt Flexibility

$$A_B = \pi(1.05^2 - 0.90^2) = 0.91 \text{ in.}^2,$$

$$L_B = 1.60 - 0.45 = 1.15 \text{ in.}$$

The axial flexibility of the bolt is

$$F_B = \frac{L_B}{A_B E_T} = 1.26/E_T.$$

The bending flexibility of the bolt is

$$= \quad F'_B = e^2 \left(\frac{\theta}{M}\right) = 1.14/E_T,$$

where

$$\frac{\theta}{M} = 19.8/E_T,$$

and

$$e = \frac{1.05 + 0.90}{2} - \frac{0.86 + 0.60}{2} = 0.24 \text{ in.}$$

Flange Flexibility

$$L_F = L_B = 1.15 \text{ in.},$$

$$A_F = \pi(0.86^2 - 0.50^2) = 1.54 \text{ in.}^2,$$

$$F_F = \frac{L_F}{A_F E_T} = 0.75/E_T.$$

Bolt Creep

The axial creep of the bolt is

$$K_B = \frac{C_1 P_t^{\,n} L_B}{A_B^{\,n}} = 1.82\, C_1 P_t^{\,4.82}.$$

In order to obtain the bending creep rate of the bolt, the stresses for an inwardly projecting flange are calculated from Reference (15). The critical combination of these stresses by the ASME Boiler Code[1] is

$$\frac{S_H + S_T}{2} = 9.18\ M.$$

For a maximum design stress equal to 2/3 σ_y = 80,000 psi, the design moment equals 80,000/9.18, or M = 8710 in-lb. With a moment arm e = 0.24 in., this corresponds to an initial nut design load of 36,300 lb. In this case, the initial load of 36,300 lb is not limited by the axial stress in the nut, but by the stress in the inwardly projecting flange.

The thickness of an equivalent loose-type flange is determined from Reference (1) using the basic geometry of the inwardly projecting flange of Figure 17. The equivalent thickness equals 0.575 in. The creep rate of the equivalent loose-type flange, calculated from Equation (6), is

$$K'_B = \frac{2\sigma_{Ft}^{\ n} C_1 e c_F}{h} = 1.26\ C_1 P_t^{4.82},$$

where

$$\sigma_{Ft} = 1.21\ P_t.$$

Flange Creep

$$K_F = \frac{C_1 P_t^{\ n} L_F}{A_F^{\ n}} = 0.145\ C_1 P_t^{4.82}.$$

Flexibility and Creep Ratios

$$r_F = 0.595, \qquad r'_F = 0.905,$$

$$r_K = 0.0796, \qquad r'_K = 0.693,$$

$$R = \frac{1 + r_F + r'_F}{1 + r_K + r'_K} = 1.41.$$

Intercept Stress Reduction

The initial bolt stress is

$$\sigma_{BR} = P/A_B = 36,300/0.91 = 40,000 \text{ psi},$$

$$\sigma_{BT} = 40,000\left(\frac{E_T}{E_R}\right) = 30,000 \text{ psi}.$$

From Equation (9),

$$\sigma_o = 24,700 \text{ psi},$$

or

$$P_o = \sigma_o A_B = 22,500 \text{ lb}.$$

Nut Relaxation

From Equation (10),

$$t = 1.18 \times 10^{18} \left[\frac{1 - \left(\frac{\sigma_t}{\sigma_o} \right)^{n-1}}{\sigma_t^{\,n-1}} \right] . \qquad (29)$$

The relaxation curve is shown in Figure 18.

External Loads

It is assumed that $K_A = K_M = 0.50$ in this example. The leakage criterion used in Equation (26) is used in Equation (19) to calculate a leakage pressure versus time curve. For example (for the connector shown in Figure 11), at a pressure p of 2000 psi, from Equation (26),

$$P_p + P_G = 33,000 \text{ lb}.$$

From Equation (20),

$$P_A = 7440 \text{ lb},$$

$$P_M = 5920 \text{ lb}.$$

Then, from Equation (19),

$$P'_t = 33,000 + 7440 + 5920 = 46,360 \text{ lb}.$$

The design curve of Figure 13 gives t = 0.37 hour. The results are shown in Figure 14 ($K_A = K_M = 0.50$, $\Delta T = 0$).

Bolt-Flange Temperature Differential

It is assumed that at the beginning of the cooling-down cycle, the bolt assembly is hotter than the flange assembly, or

$$\Delta T = -100 \text{ F}.$$

From Equation (21) and the geometry of Figure 11,

$$\Delta\sigma_B = \frac{\alpha(\Delta T)E_T}{1 + r_F} = 11,000 \text{ psi.}$$

The reduction in bolt load due to the thermal gradient is

$$P_T = (11,000)(1.89) = 20,800 \text{ lb.}$$

From Equation (23),

$$P'_t = P_p + P_G + P_T. \tag{30}$$

From Equations (26) and (30), at a pressure p = 1500 psi,

$$P'_t = \pi(1500)(1.95^2) + 3(1500)(1.53) + 20,800 = 45,580 \text{ lb.}$$

From Figure 13, t = 0.52 hour.

The results of the analysis are shown in Figure 14 ($K_A = K_M = 0$, $\Delta T = -100$ F).

APPENDIX B

DERIVATION OF EQUATIONS

APPENDIX B

DERIVATION OF EQUATIONS

Flange Flexibility

Loose Type

Timoshenko[18] gives the flange rotation θ_F due to a flange moment M as

$$\theta_F = \frac{12M}{2\pi E_T h^3 \ln d_F/c_F} . \tag{31}$$

Since

$$M = Pe,$$

and the flange deflection at the bolt circle is

$$\delta_F = e\theta_F, = \frac{1.91Pe^2}{E_T h^3 \ln d_F/c_F} \tag{32}$$

then,

$$F_F = \frac{2\delta_F}{P} = \frac{3.82e^2}{E_T h^3 \ln d_F/c_F} . \tag{33}$$

Integral Type

Wesstrom and Bergh[17] present an equation for the flange rotation:

$$\theta_F = \frac{0.645\ VM}{L\sqrt{c_F}\ (d_T - c_T)^{5/2} E_T} . \tag{34}*$$

Since the total flange moment M = Pe, and the deflection $\delta_F = \theta_F e$,

$$F_F = \frac{2\delta_F}{P} \quad \frac{1.29\ Ve^2}{L\sqrt{c_F}(d_T - c_T)^{5/2} E_T} . \tag{35}*$$

*The terms V and L in Equations (34) and (35) conform to the nomenclature of Reference (1).

Bolt Creep

From the steady-state creep law,

$$\epsilon_B = C_1 \sigma_B^{\,n} t, \tag{36}$$

or, the bolt deflection is

$$\delta_B = \frac{C_1 P_t^{\,n} t L_B}{A_B^{\,n}}, \tag{37}$$

where

$$\sigma_B = \frac{P_t}{A_B}.$$

Then,

$$K_B = \frac{\delta_B}{t} \quad \frac{C_1 P_t^{\,n} L_B}{A_B^{\,n}} \tag{38}$$

Flange Creep

Marin[19] developed equations for the steady-state creep of a circular ring of rectangular cross section subjected to uniform moments. The flange rotation and maximum stress on the inner surface are

$$\theta_F = \left[\left(\frac{P_t e}{2\pi} \right) \frac{\left(2^{1+\frac{1}{n}}\right)\left(1-\frac{1}{n}\right)\left(2+\frac{1}{n}\right)}{\left(d_F^{\,1-\frac{1}{n}} - c_F^{\,1-\frac{1}{n}}\right) h^{2+\frac{1}{n}}} \right]^n C_1 t, \tag{39}$$

$$\sigma_{Ft} = \left(\frac{h}{2c_F} \right)^{\frac{1}{n}} \left(\frac{P_t e}{2\pi} \right) \left[\frac{\left(2^{1+\frac{1}{n}}\right)\left(1-\frac{1}{n}\right)\left(2+\frac{1}{n}\right)}{\left(d_F^{\,1-\frac{1}{n}} - c_F^{\,1-\frac{1}{n}}\right) h^{2+\frac{1}{n}}} \right]. \tag{40}$$

Equations (39) and (40) are based on the steady-state creep law $\epsilon = C_1 \sigma^n t$ and assume the creep stress distribution in the flange. There exists sufficient test and theoretical data on the creep bending of beams[20, 21, 22, 23, 24] to justify that:

(1) Plane sections remain plane.

(2) The creep deflections can be predicted on the basis of the steady-state creep law.

(3) Individual fibers of the beam creep at a rate equivalent to that predicted by a tensile creep test.

(4) The creep stress distribution is attained shortly after the commencement of the test and does not change for the remainder of the test. This is analytically confirmed by Hult[24]. Because of the like nature of the beam and ring deformations, the above assumptions are also assumed to hold true for the creep deflection of a flange.

From Equations (39) and (40),

$$\theta_F = \frac{2\sigma_{Ft}^{\ n} C_1 c_F t}{h} . \tag{41}$$

Then,

$$K_F = \frac{2e\theta_F}{t} = \frac{4\sigma_{Ft}^{\ n} C_1 e c_F}{h} . \tag{42}$$

Intercept Stress Reduction

It is assumed that the initial stress σ_{BT} is reduced in zero time to a new value σ_o which has a total intercept strain ϵ_o equal to the initial bolt stress σ_{BT} divided by the modulus of elasticity E_T. From Figure 19,

$$\epsilon_o = \epsilon_e + C_2\sigma_o^{\ m} , \tag{43}$$

or

$$\sigma_{BT} = \sigma_o + E_T C_2 \sigma_o^{\ m} . \tag{44}$$

The constants C_2 and m are determined by a best fit to the intercept data from a family of creep curves at the design temperature.

For a flexible flange, the interaction of the flange and bolt has to be accounted for. The primary creep of the bolt can be represented by

$$\delta_{Bc} = C_2\sigma_o^{\ m} L_B . \tag{45}$$

The change in bolt stress is determined by the elastic bolt recovery:

$$\sigma_o = \sigma_{BT} - \frac{\delta_{Be} E_T}{L_B} . \tag{46}$$

From Figure (20), in order to maintain compatibility of bolt and flange,

$$\delta_{TOTAL} = \delta_{Fe} - \delta_{Fc} = \delta_{Bc} - \delta_{Be} \cdot \tag{47}$$

By definition,

$$r_F = \frac{\delta_{Fe}}{\delta_{Be}}, \quad r_K = \frac{\delta_{Fc}}{\delta_{Bc}}$$

$$R = \frac{1 + r_F}{1 + r_K},$$

and Equation (47) becomes

$$\delta_{Be}(r_F + 1) = \delta_{Bc}(r_K + 1), \tag{48}$$

or

$$\frac{\delta_{Be}}{\delta_{Bc}} = \frac{1 + r_K}{1 + r_F} = \frac{1}{R} . \tag{49}$$

Substituting (45) and (46) in (49),

$$\sigma_o = \sigma_{BT} - \frac{E_T C_2 \sigma_o^{\,m}}{R} . \tag{50}$$

For a rigid flange (R = 1), Equation (50) is identical to Equation (44). The development of Equation (50) for a flexible flange assumes that the creep ratio r_K is the same for primary creep as it is for steady-state creep.

Bolt Relaxation

The analysis of bolt relaxation is similar to that of References (2, 6). The nomenclature is defined as follows:

L_F = original length between nut bearing surfaces

L_B = length of bolt if it is relieved of stress before creep occurs

$\delta' = L_F - L_B$ = initial flange deflection plus bolt extension (or total initial relative movement between nut and bolt)

$K_F t = \delta_{Fc}$ = creep deflection of flanges

$K_B t = \delta_{Bc}$ = creep deflection of bolts

$F_F P = \delta_{Fe}$ = elastic flange deflection

$F_B P = \delta_{Be}$ = elastic bolt deflection.

In order that the flange and bolts maintain contact at any time,

$$L_F - \delta_{Fc} - \delta_{Fe} = L_B + \delta_{Bc} + \delta_{Be}\,, \tag{51}$$

or

$$\delta' = \delta_{Bc}\,(1 + r_K) + \delta_{Be}\,(1 + r_F). \tag{52}$$

Since

$$\delta_{Be} = \frac{\delta_B L_B}{E_T}\,,$$

$$\delta' = \delta_{Bc}\,(1 + r_K) + \frac{\delta_B L_B}{E_T}\,(1 + r_F),$$

or

$$\sigma_B = \frac{E_T}{L_B}\left[\frac{\delta' - \delta_{Bc}\,(1 + r_K)}{1 + r_F}\right]. \tag{53}$$

Differentiate (53) with respect to time:

$$\frac{d\sigma_B}{dt} = \frac{-E_T}{L_B}\left(\frac{1 + r_K}{1 + r_F}\right)\frac{d\delta_{Bc}}{dt}\,. \tag{54}$$

From the steady-state creep law,

$$\dot{\epsilon}_c = C_1\sigma_B^{\,n} = \frac{d\epsilon_c}{dt} = \frac{d}{dt}\left(\frac{\delta_{Bc}}{L_B}\right),$$

or

$$\frac{d\delta_{Bc}}{dt} = L_B C_1 \sigma_B^{\,n}\,. \tag{55}$$

Substitute (55) in (54):

$$\frac{d\sigma_B}{\sigma_B^{\,n}} = \frac{-E_T C_1\,dt}{R}\,. \tag{56}$$

Integrate (56), letting $\sigma_B = \sigma_t$:

$$\frac{\sigma_t^{\,-n+1}}{1-n} = \frac{-E_T C_1 t}{R} + C, \tag{57}$$

where C is a constant of integration. At $t = 0$, $\sigma_t = \sigma_o$. Therefore,

$$C = \frac{\sigma_o^{-n+1}}{1-n} .$$

From (57),

$$t = \frac{R}{C_1 E_T (n-1)} \left[\frac{1 - \left(\frac{\sigma_t}{\sigma_o}\right)^{n-1}}{\sigma_t^{n-1}} \right] . \quad (58)$$

Equation (58) also applies to the relaxation of the nut in a threaded connector design with R defined by Equation (18).

External Loads

Axial Load

The axial load P_A is assumed to be a tensile force which reduces the gasket pressure. The magnitude of the tube stress σ_A due to the axial load P_A is defined as a constant times the axial tube stress due to internal pressure:

$$P_A = \sigma_A A_T = \sigma_A \pi \left(d_T^2 - c_T^2 \right), \quad (59)$$

where

$$\sigma_A = K_A \sigma_T = \frac{p K_A c_T^2}{\left(d_T^2 - c_T^2 \right)} . \quad (60)$$

From (59) and (60),

$$P_A = \pi p K_A c_T^2 \quad (61)$$

Bending Moment

The required additional bolt load P_M accounts for the tendency of the tube bending moment M_T to reduce the gasket pressure. The magnitude of the tube stress σ_M due to the bending moment M_T is defined as a constant K_M times the axial tube stress due to internal pressure:

$$\sigma_M = K_M \sigma_T = \frac{p K_M c_T^2}{\left(d_T^2 - c_T^2 \right)} . \quad (62)$$

From beam bending theory,

$$\sigma_M = \frac{4 M_T d_T}{\pi \left(d_T^4 - c_T^4 \right)} . \quad (63)$$

Combining (62) and (63),

$$M_T = \frac{\pi_p K_M c_T^2 (d_T^2 + c_T^2)}{4d_T} \quad . \tag{64}$$

The bending moment M_T is considered to reduce the gasket pressure by the amount σ_G on one side of the gasket. If the gasket width is assumed small compared to the gasket radius,

$$\sigma_G = \frac{M_T}{\pi g^2 w} = \frac{p K_M c_T^2 (d_T^2 + c_T^2)}{4 d_T g^2 w} \quad . \tag{65}$$

If the maximum gasket pressure is assumed to act on the complete gasket surface,

$$P_M = A_G \sigma_G = 2\pi g w \sigma_G = \frac{\pi p K_M c_T^2 (d_T^2 + c_T^2)}{2 d_T g} \quad . \tag{66}$$

Bolt-Flange Temperature Differential

The thermal bolt strain $\Delta\epsilon_B = \alpha(\Delta T)$ corresponds to a thermal bolt deflection $\Delta L_B = \alpha(\Delta T) L_B$ which is distributed according to the flexibility of the flange and bolt. From Figure 20,

$$\alpha(\Delta T) L_B = \delta_{Fe} + \delta_{Be} = \delta_{Be} (r_F + 1). \tag{67}$$

The change in bolt stress is

$$\Delta\sigma_B = \left(\frac{\delta_{Be}}{L_B}\right) E_T \quad . \tag{68}$$

From (67) and (68),

$$\Delta\sigma_B = \frac{\alpha(\Delta T) E_T}{1 + r_F} \quad . \tag{69}$$

Following a similar procedure for the threaded connector,

$$\Delta\sigma_B = \frac{\alpha(\Delta T) E_T}{1 + r_F + r'_F} \quad . \tag{70}$$

APPENDIX C

SECONDARY EFFECTS

APPENDIX C

SECONDARY EFFECTS

Stress Concentrations

Because of the accelerated rate of creep at higher stress levels, the presence of stress concentrations such as bolt threads might be expected to increase the over-all creep rates of the assembly. However, the results of the British Flange Tests(9) indicate that the creep of the nut assembly was not exceedingly high if the nut material was equivalent to the bolt material. However, when carbon steel nuts were used with alloy steel bolts, the creep of the nut assembly was excessive.

A comprehensive review of stress concentrations under creep conditions was presented in Reference (25). The strength of a specimen with a notch under creep conditions is attributed partly to the ability of the material in the notch area to flow rapidly and redistribute stresses at high temperatures; also because the greater volume of lower stressed material away from the notch restrains the over-all deformations.

Creep Bending of Bolt

The tendency of the bolt in a flanged joint assembly to develop bending moments due to flange rotations and shifting of the nut reaction is well known. Under creep conditions, however, the stress distribution becomes more favorable because of the redistribution of the bending stresses. Bailey(3) developed a solution, based on the steady-state creep law, for the creep stresses due to combined axial and bending loads on a rectangular cross section; the results are shown in Figure 21. The results for a solid circular section should be comparable because of the relative values of the plastic bending factor for the rectangular and solid circular sections.

Dynamic Creep

Superimposed alternating stresses are known to affect the creep rate of metals. However, Lazan(26) showed that the presence of alternating stresses did not appear to affect greatly the creep rate for most materials. Results for Waspaloy at 1500 F from Reference (27) are shown in Figure 22.

Langenecker(28) has recently discussed a problem of possible significance to connectors operating in a high acoustic radiation field. He found that intense ultrasound could have a marked effect on the physical properties of solids.

Gasket Creep*

The gasket will contribute a certain amount of creep and flexibility to the connector assembly. This contribution is neglected in the design procedure in view of the relatively short length of the gasket in most designs. Also, for metallic gaskets, the stresses in the gasket are usually lower than those of the bolt assembly. In fact, the gasket area should be chosen, on the basis of the relative creep strengths of the gasket and bolt material, such that the creep rate of the gasket is negligible. The inclusion of the gasket creep and flexibility properties in the design procedure will unduly complicate the equations, with very little gain in design accuracy for most geometries.

Flange Rotations

Changes in the flange rotation and corresponding bolt-load changes due to the application of internal pressure are neglected in the design procedure. These effects are considered secondary from the standpoint of over-all bolt relaxation, but should be considered in the static design of the connector if found to be significant.

* The design procedure could be extended to include the effects of gasket creep in an approximate, but quite conservative manner.

APPENDIX D

TUBE DESIGN

APPENDIX D

TUBE DESIGN

The tube design is considered on page 18 only to the extent that it affects the strength of the connector. The tube, however, is subjected to progressive creep deformations with each operating cycle. The tube thickness should satisfy the minimum requirements for a creep design. Some of the appropriate theories available for the tube creep design are reviewed below.

Finnie and Heller[7] present the equation for the tangential strain rate in a thin-walled tube with closed ends under internal pressure:

$$\dot{\epsilon}_\phi = C_1 \left(\frac{pc_T}{d_T - c_T}\right)^n \left(\frac{3}{4}\right)^{\frac{n+1}{2}} = \dot{\epsilon}\left(\frac{3}{4}\right)^{\frac{n+1}{2}} , \tag{71}$$

where $\dot{\epsilon} = C_1\sigma^n$ = the strain rate which would be produced by the tangential stress

$$\sigma = \frac{pc_T}{d_T - c_T}$$

acting alone in simple tension.

The creep of thin-walled tubes under internal pressure, axial loads, and moments is considered in Reference (7).

Finnie and Heller[7] also analyzed the creep of thick-walled tubes subjected to internal pressure. Based on the Mises flow law and the steady-state creep law $\dot{\epsilon} = C_1\sigma^n$, the radial, tangential, and axial stresses, respectively, are

$$\sigma_r = -p\frac{\left(\frac{d_T}{r}\right)^{2/n} - 1}{\left(\frac{d_T}{c_T}\right)^{2/n} - 1} ,$$

$$\sigma_\phi = p\frac{\left(\frac{2-n}{n}\right)\left(\frac{d_T}{r}\right)^{2/n} + 1}{\left(\frac{d_T}{c_T}\right)^{2/n} - 1} , \tag{72}$$

$$\sigma_z = p\frac{\left(\frac{1-n}{n}\right)\left(\frac{d_T}{r}\right)^{2/n} + 1}{\left(\frac{d_T}{c_T}\right)^{2/n} - 1} ,$$

where

r = variable radius, $c_T \leq r \leq d_T$.

Equations (72) reduce to the well-known Lamé formulas for n = 1. The tangential strain rate is

$$\dot{\epsilon}_\phi = C_1 \left(\frac{3}{4}\right)^{\frac{n+1}{2}} \left[\frac{p}{\left(\frac{d_T}{c_T}\right)^{2/n} - 1} \left(\frac{2}{n}\right) \right]^n \left(\frac{d_T}{r}\right)^2 . \qquad (73)$$

The steady-state creep stresses and strain rates in a thick-walled tube under combined internal pressure and axial load are presented by Finnie[29]. Numerical solutions to the equations are tabulated for various values of the variables. In the case where the additional axial load is either small or large compared to the axial load due to internal pressure, simple approximate solutions are given. Finnie[30] also pointed out the lack of complete agreement between the theoretical and experimental studies on multiaxial creep in tubes, attributing the discrepancies to the effect of hydrostatic stress which is usually assumed negligible in creep strain predictions.

A method for predicting the creep failure time for either thin-walled or thick-walled circular cylinders can be found in Reference (31). True stress and true strain are used and the steady-state creep law is assumed valid until failure. The failure time is based on plastic instability, or the time at which the vessel wall is no longer sufficient to hold the load. Simplified formulas are obtained for both thin-walled and very-thick-walled cylinders.

Creep-rupture tests[32] were run on Type 316 stainless steel tubes at high temperatures and pressures. The results of the tests compare favorably with those of uniaxial tension tests if effective stress and effective strain rate are used. Rattinger and Padlog[33] also present a method of analysis for predicting creep rupture of cylindrical shells using conventional uniaxial creep data.

A method of analysis[34] for predicting the stresses and strains in thick-walled cylinders considers primary as well as secondary creep. The analysis is quite complicated and justifies a computer solution.

Equations (71) and (73) result in quite favorable strain rates for higher values of the exponent n. On this basis, the design procedure of the ASME Boiler Code[1], which compares the maximum design stress to the creep rate or rupture stress of a uniaxial tension test, provides for a safe design.

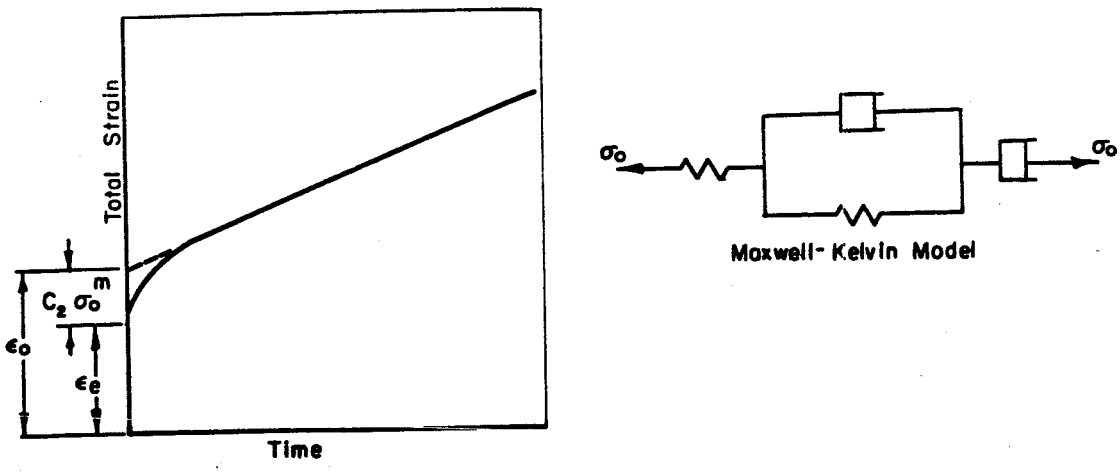

FIGURE 1. TYPICAL CREEP CURVE

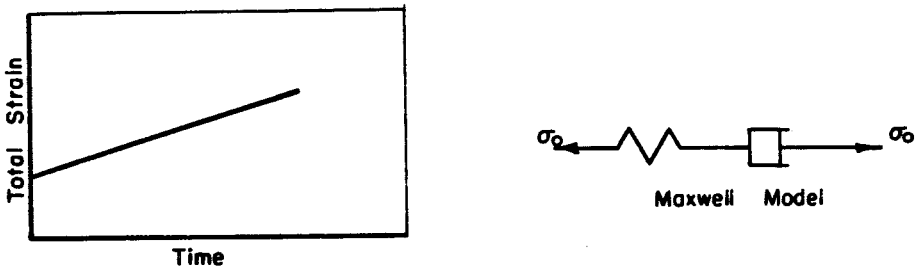

FIGURE 2. STEADY-STATE CREEP

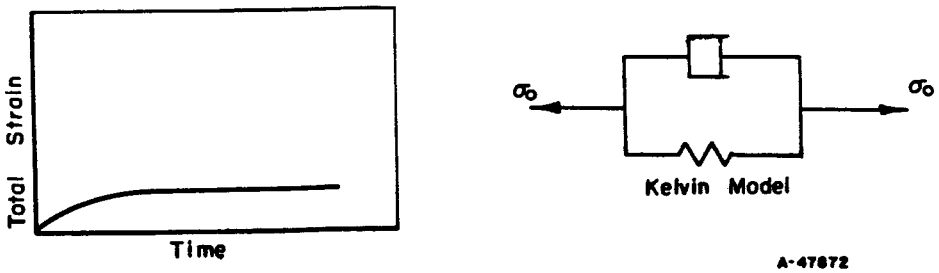

FIGURE 3. PRIMARY CREEP

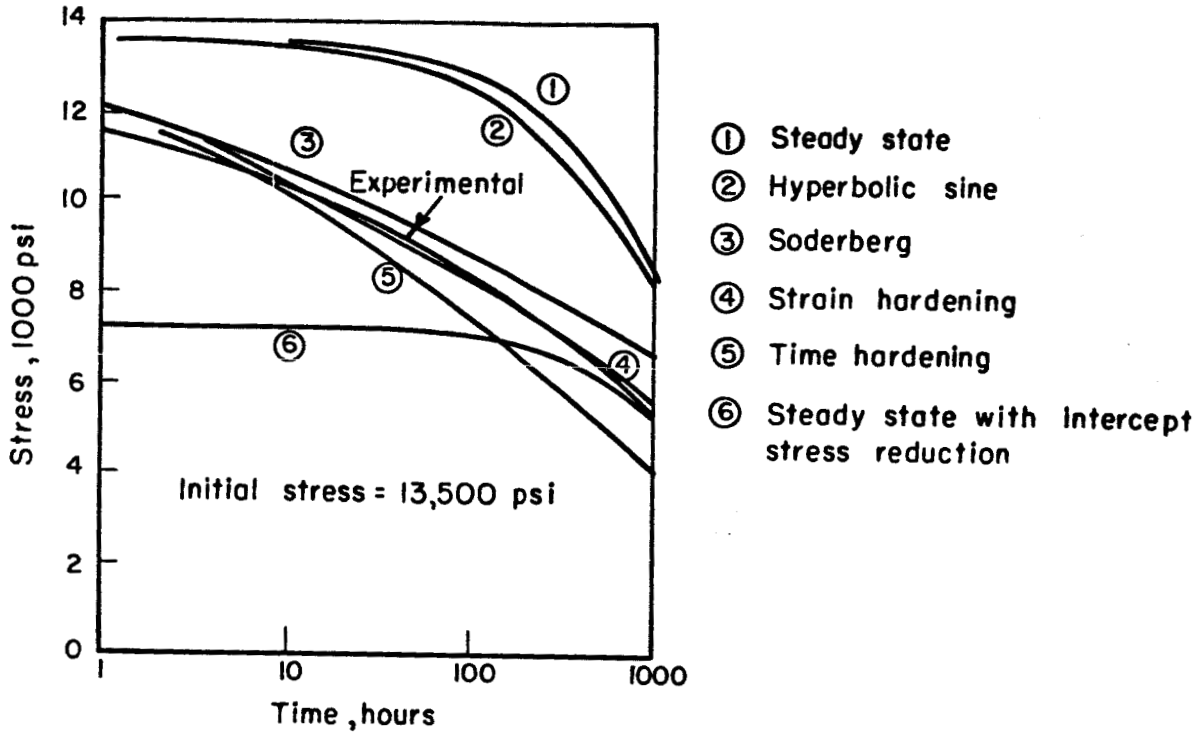

FIGURE 4. CREEP-RELAXATION COMPARISON (COPPER AT 165 C)

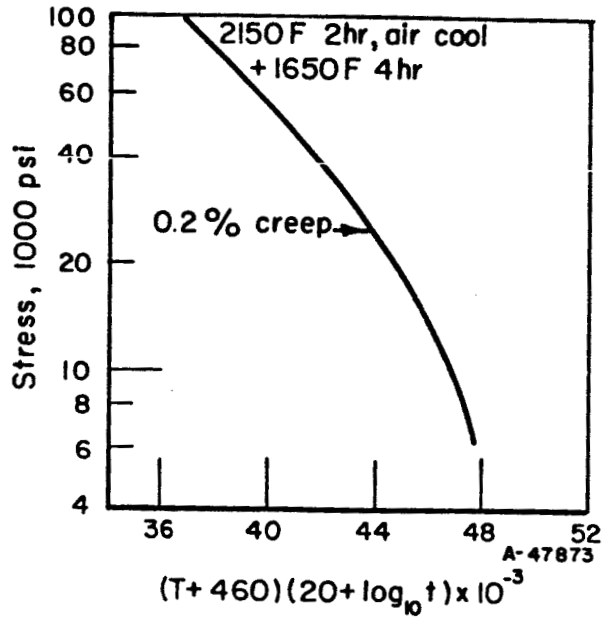

FIGURE 5. MASTER CREEP CURVE FOR RENÉ 41 BAR

BATTELLE MEMORIAL INSTITUTE

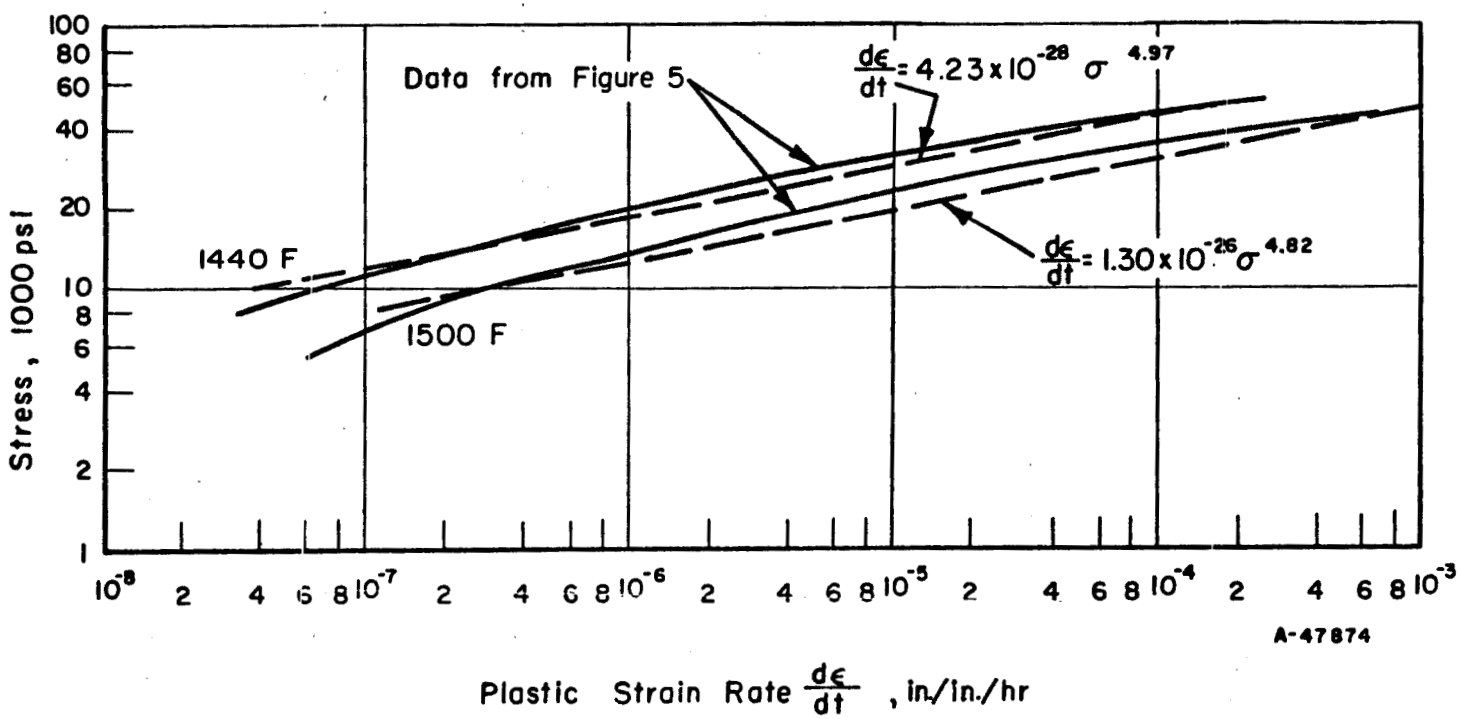

FIGURE 6. CREEP RATE OF RENÉ 41 AT 1440 F AND 1500 F

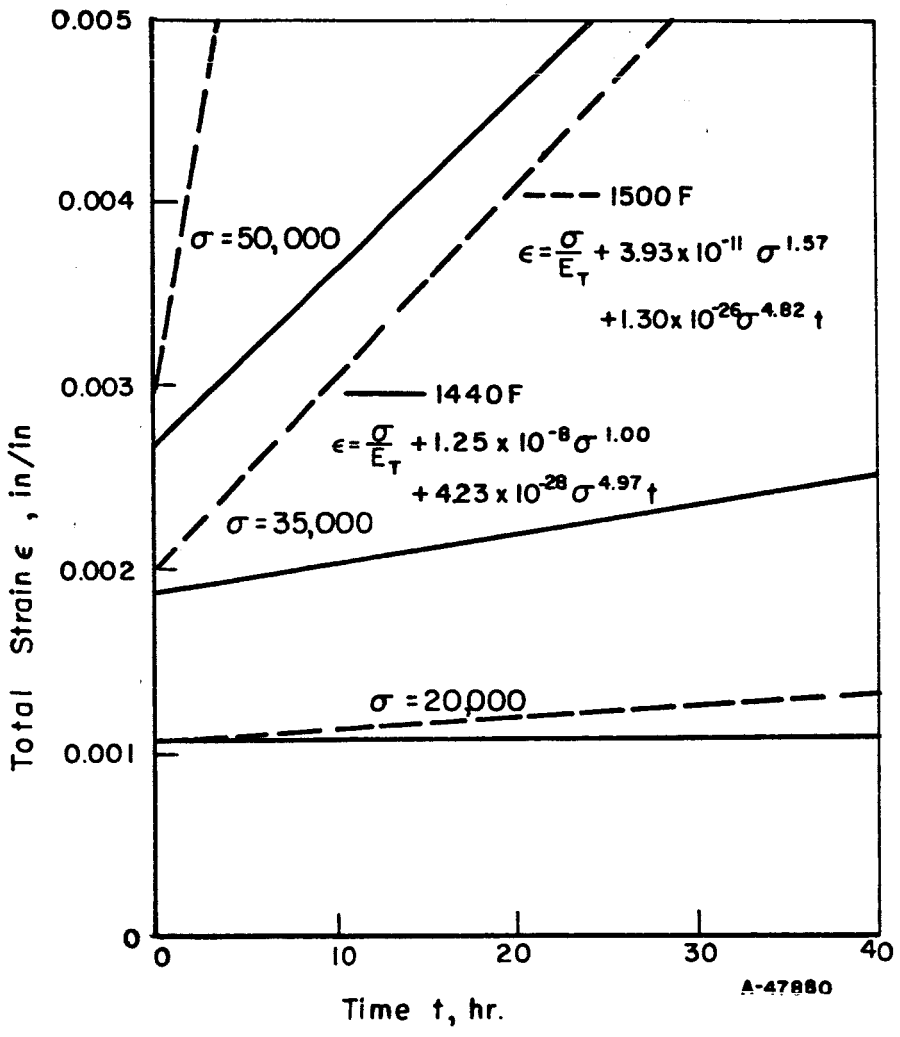

FIGURE 7. DESIGN CREEP PROPERTIES OF RENÉ 41

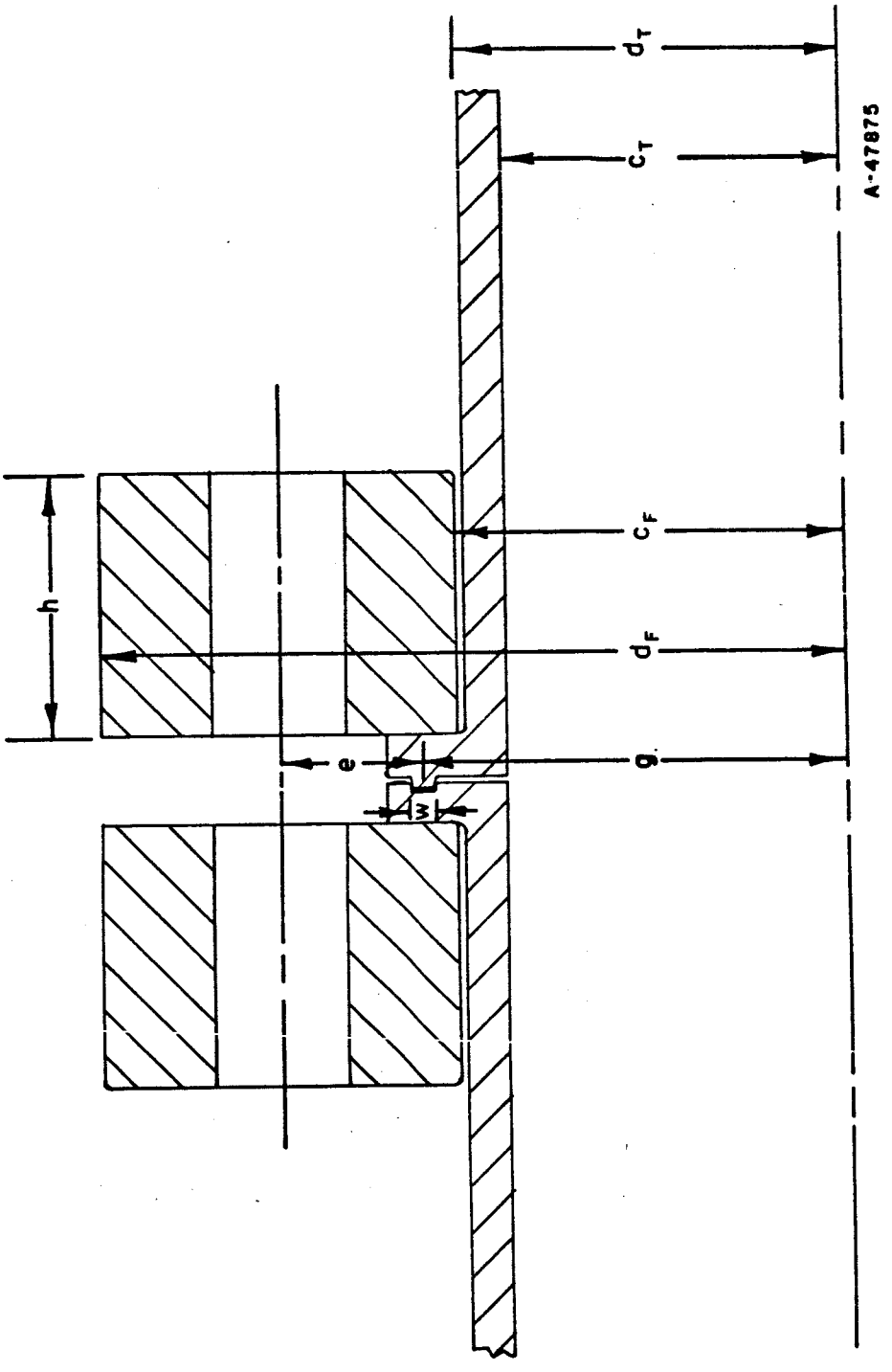

FIGURE 8. TYPICAL FLANGE GEOMETRY

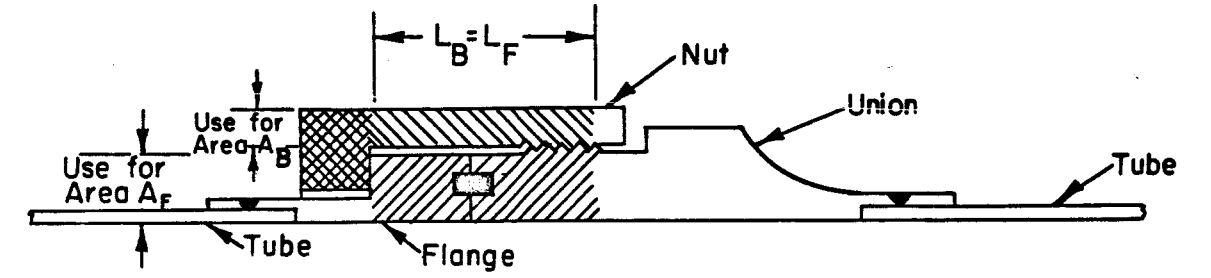

Considered as "bolt" axial deformations in analysis

Considered as "bolt" bending deformations in analysis

Considered as "flange" axial deformations in analysis

FIGURE 9. THREADED CONNECTOR MODEL

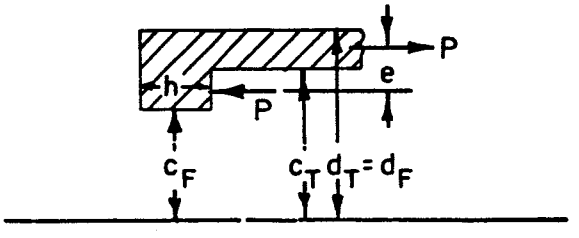

A-47879

FIGURE 10. INWARDLY PROJECTING FLANGE

BATTELLE MEMORIAL INSTITUTE

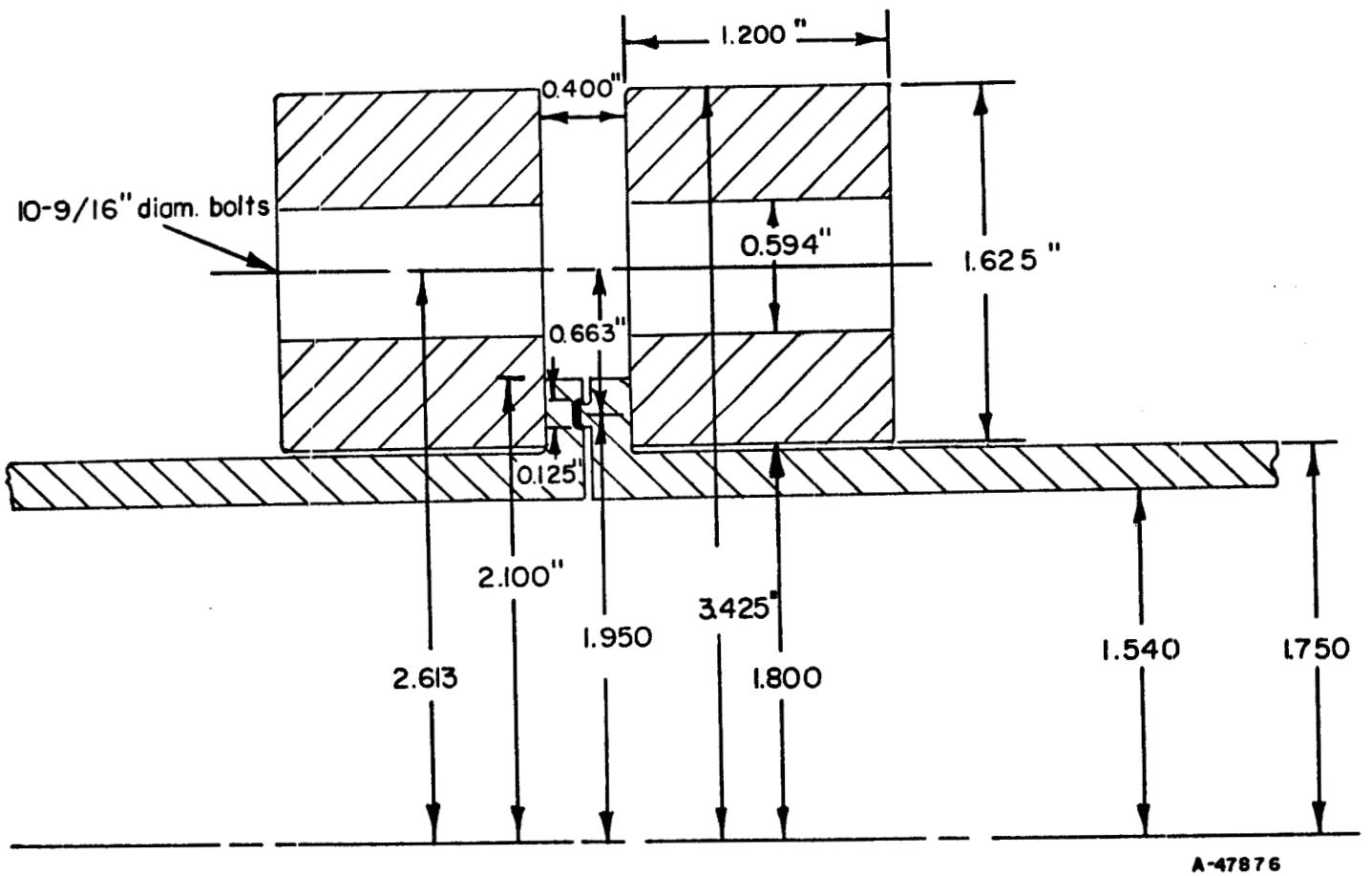

FIGURE 11. LOOSE-TYPE FLANGE GEOMETRY (RENÉ 41 - 1500 F)

BATTELLE MEMORIAL INSTITUTE

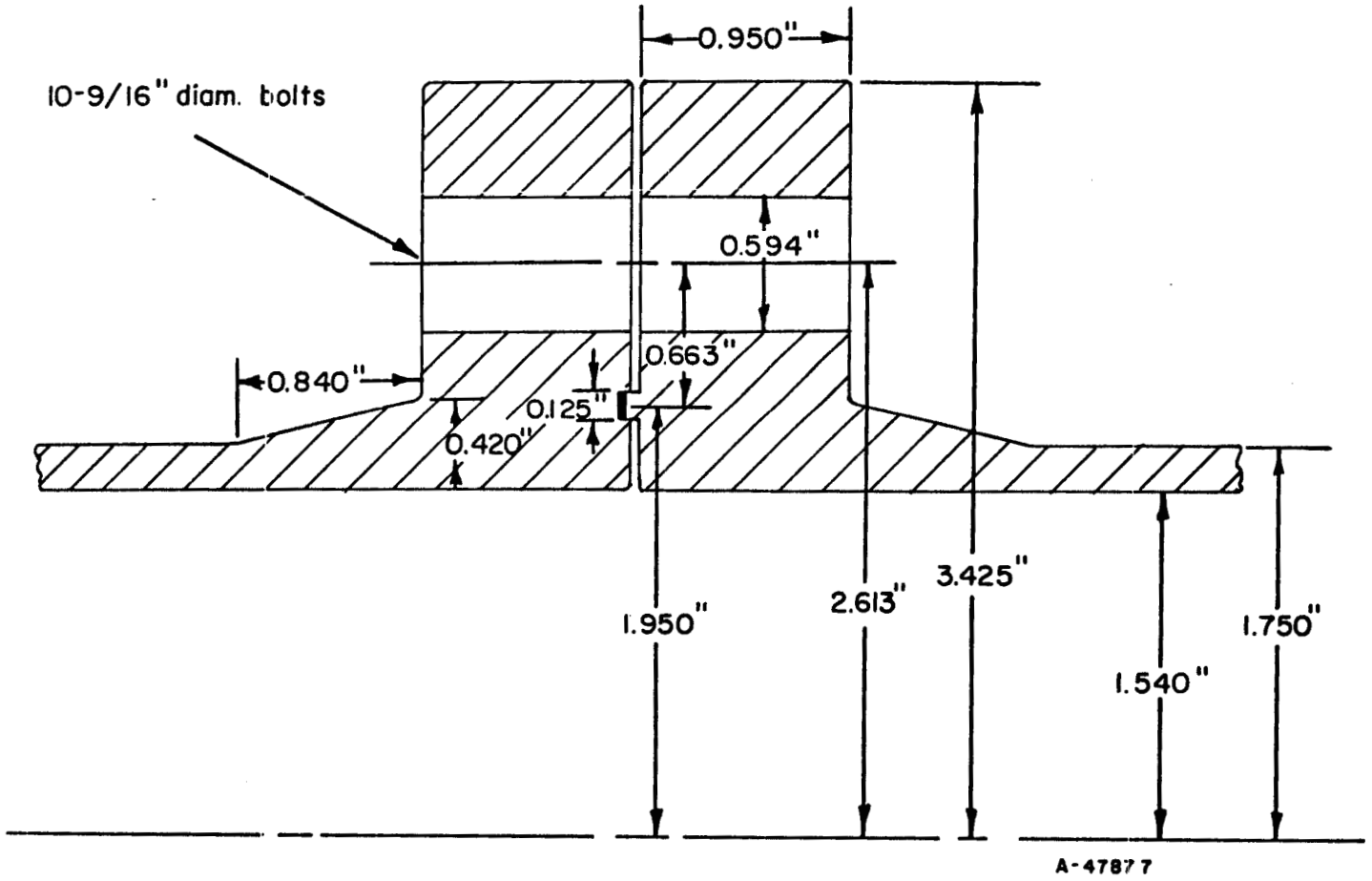

FIGURE 12. INTEGRAL-TYPE FLANGE GEOMETRY (RENÉ 41 - 1500 F)

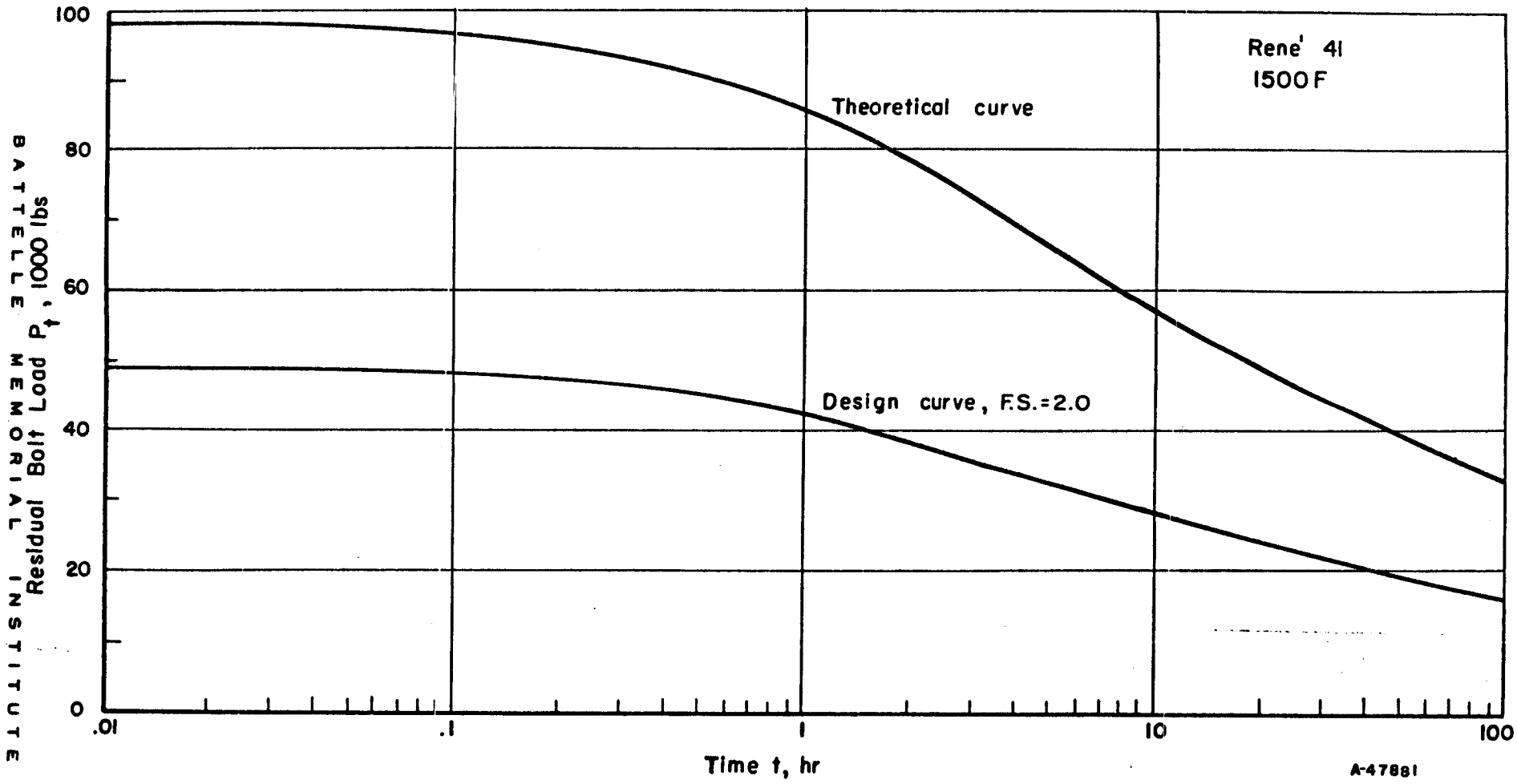

FIGURE 13. RESIDUAL BOLT LOAD VERSUS TIME FOR BOLTED-FLANGED CONNECTOR (SHOWN IN FIGURE 11)

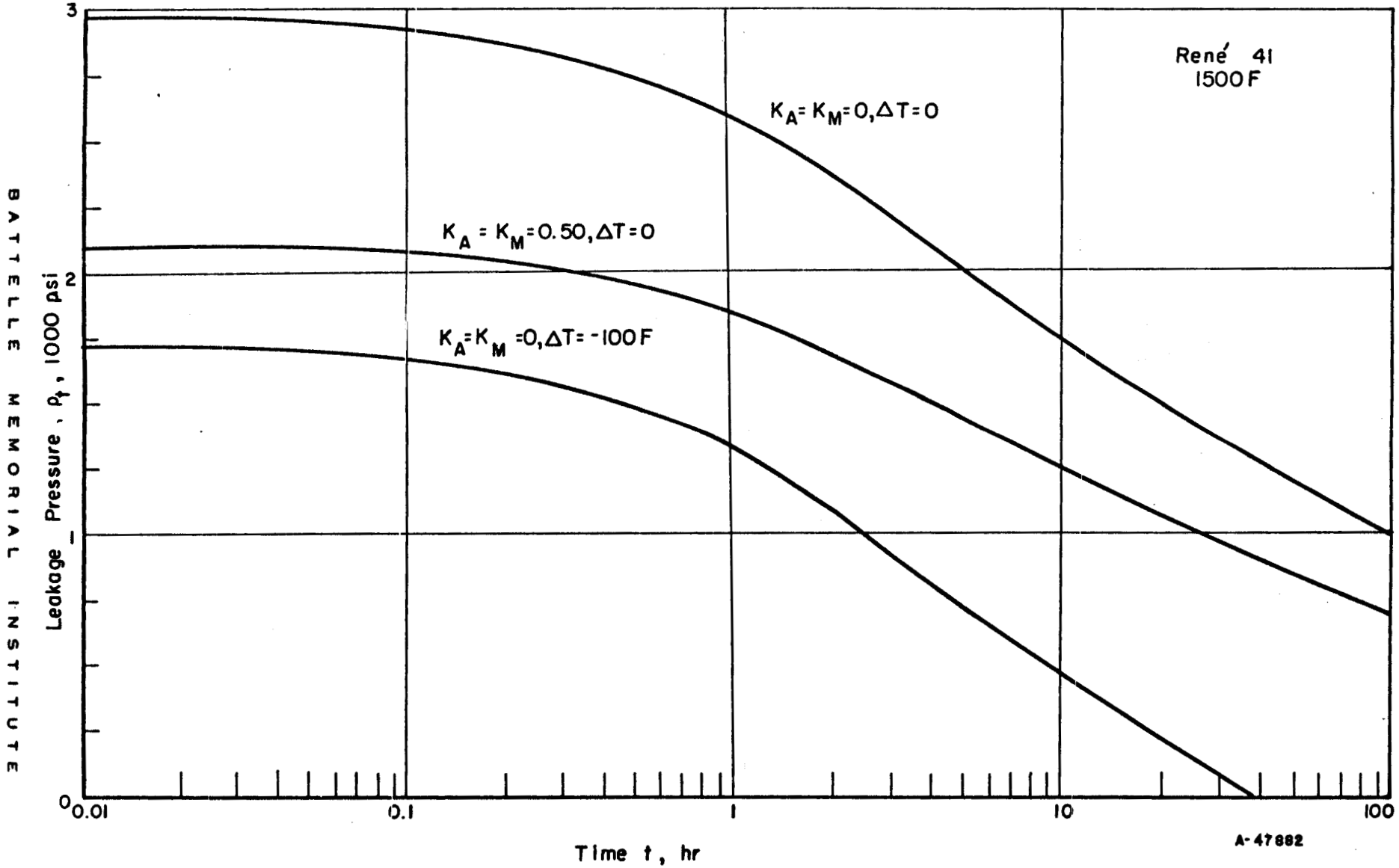

FIGURE 14. LEAKAGE PRESSURE VERSUS TIME FOR BOLTED-FLANGED CONNECTOR (SHOWN IN FIGURE 11)

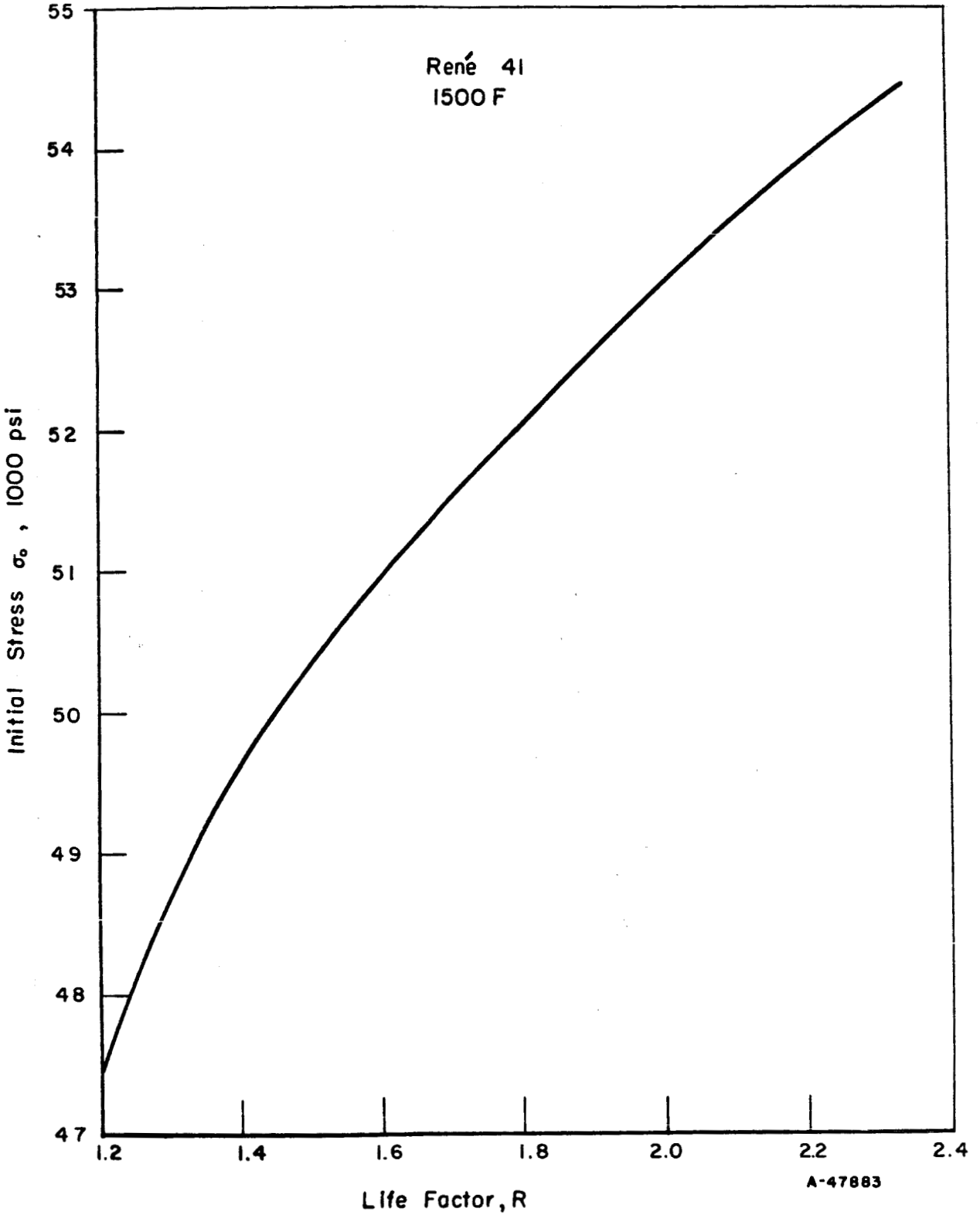

FIGURE 15. EFFECT OF LIFE FACTOR ON INITIAL STRESS (σ_{BT} = 65,400 PSI)

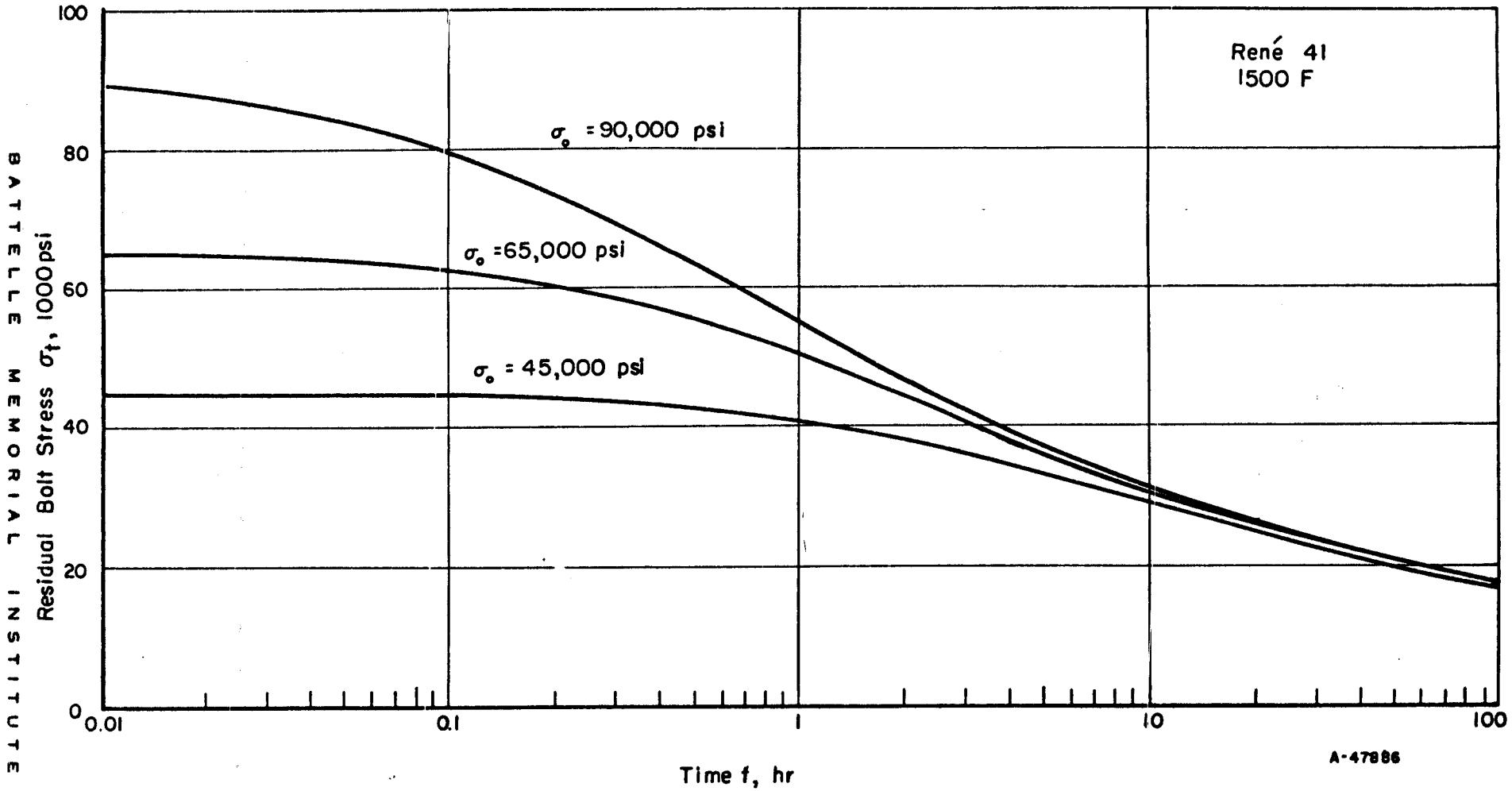

FIGURE 16. EFFECT OF INITIAL BOLT STRESS ON RELAXATION
(FLANGE GEOMETRY OF FIGURE 11)

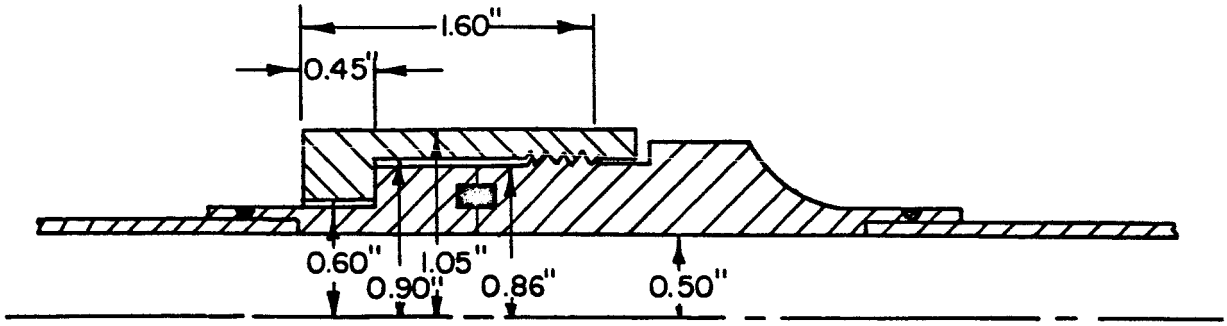

FIGURE 17. THREADED-CONNECTOR GEOMETRY

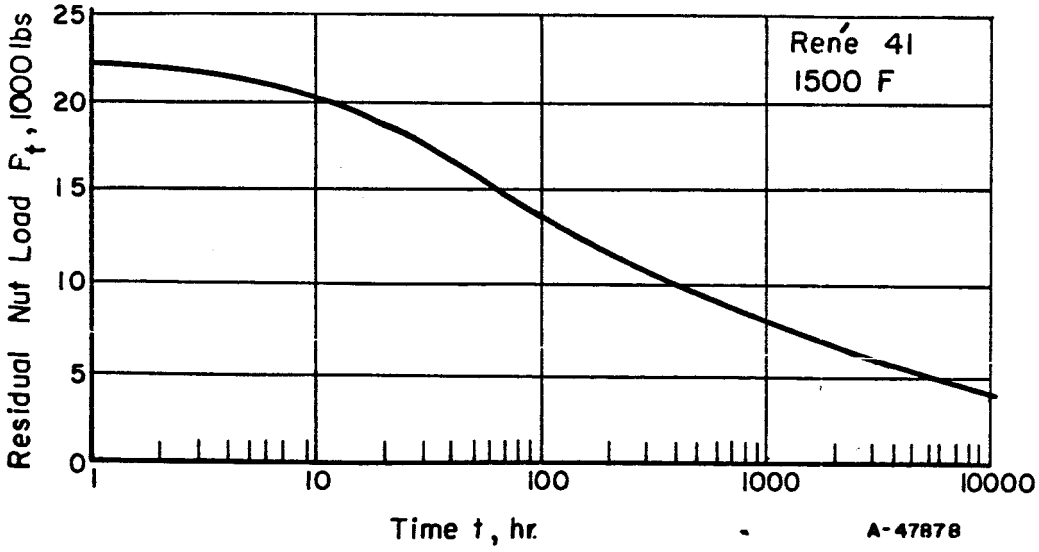

FIGURE 18. RESIDUAL NUT LOAD VERSUS TIME FOR THREADED CONNECTOR (SHOWN IN FIGURE 17)

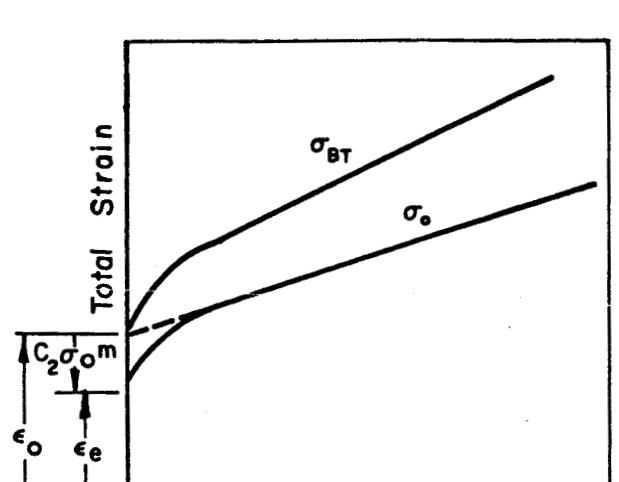

FIGURE 19. INTERCEPT STRESS REDUCTION

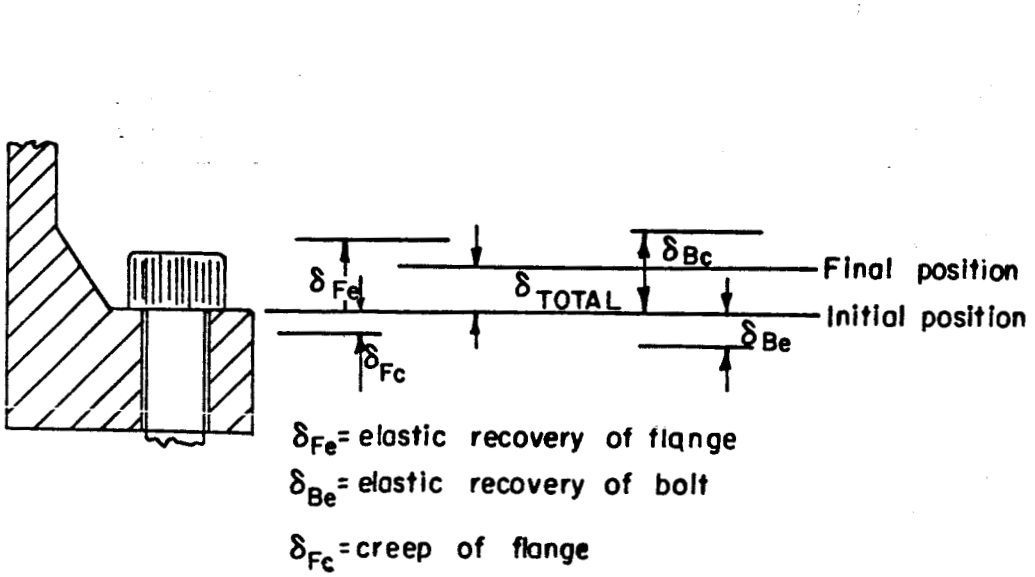

FIGURE 20. CREEP OF FLANGE AND BOLT

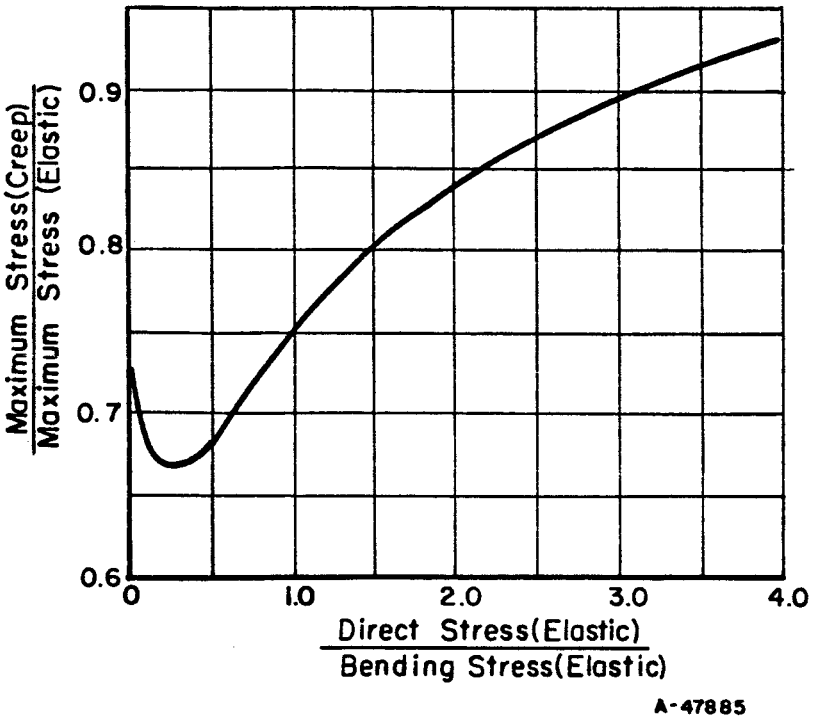

FIGURE 21. CREEP BENDING OF RECTANGULAR SECTION (n = 6)

BATTELLE MEMORIAL INSTITUTE

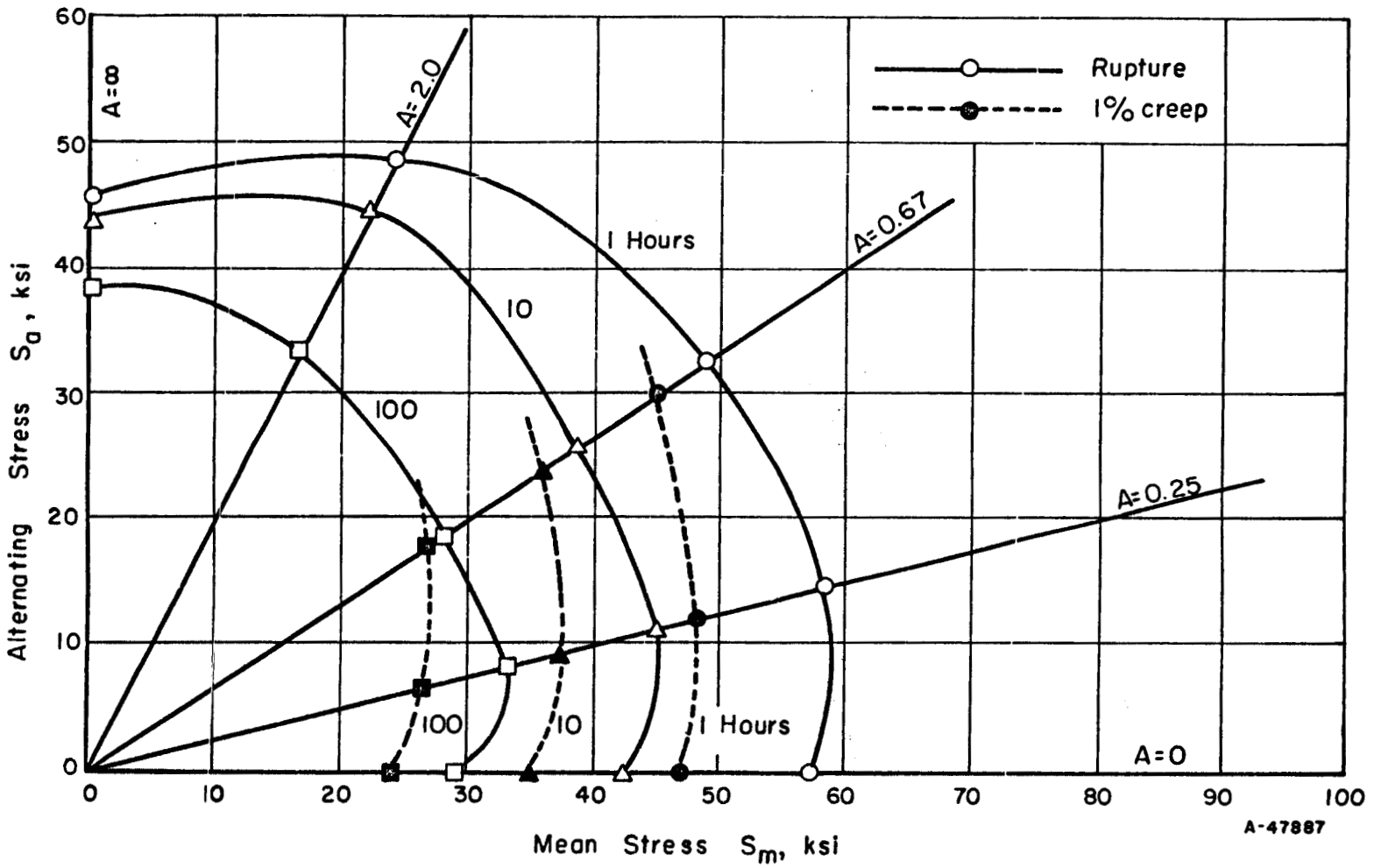

FIGURE 22. COMBINED CREEP AND FRACTURE STRESS RANGE DIAGRAM FOR 6.3% Mo-WASPALLOY AT 1500 F